MAFELAP 2006

High Accuracy Simulations of 2D and 3D Resistivity Logging Instruments Using a Self-Adaptive Goal-Oriented hp-FEM

David Pardo (dzubiaur@gmail.com),
M. Paszynski, C. Torres-Verdin, L. Demkowicz

Collaborators: J. Kurtz, L.E. Garcia-Castillo, C. Michler

Brunel University, Uxbridge, England

June 14, 2006

Department of Petroleum and Geosystems Engineering, and
Institute for Computational Engineering and Sciences (ICES)

THE UNIVERSITY OF TEXAS AT AUSTIN

OVERVIEW

1. Motivation: Simulation of Resistivity Logging Instruments.
2. Maxwell's Equationns.
3. Methodology:
   - The hp-Finite Element Method (FEM) - Exponential Convergence -.
   - Automatic Goal-Oriented Refinements - in the Quantity of Interest -.
   - Perfectly Matched Layers (PML).
4. Numerical Results:
   - Simulation of 2D Resistivity Logging Instruments.
   - Simulation of 3D Resistivity Logging Instruments.
5. Conclusions and Future Work.

RESISTIVITY LOGGING INSTRUMENTS

Logging Instruments: Definition

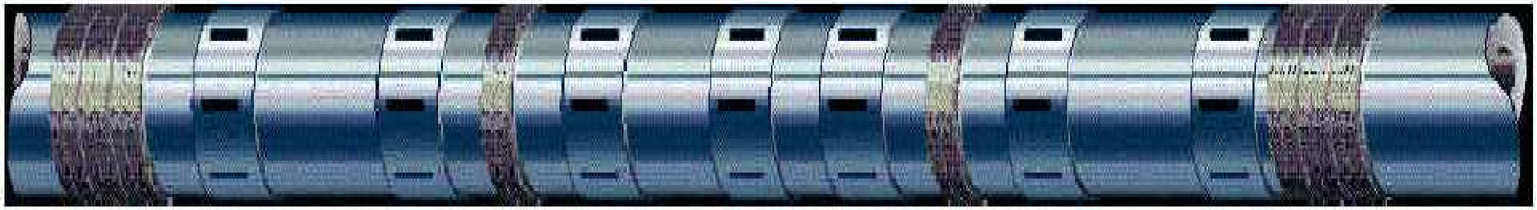

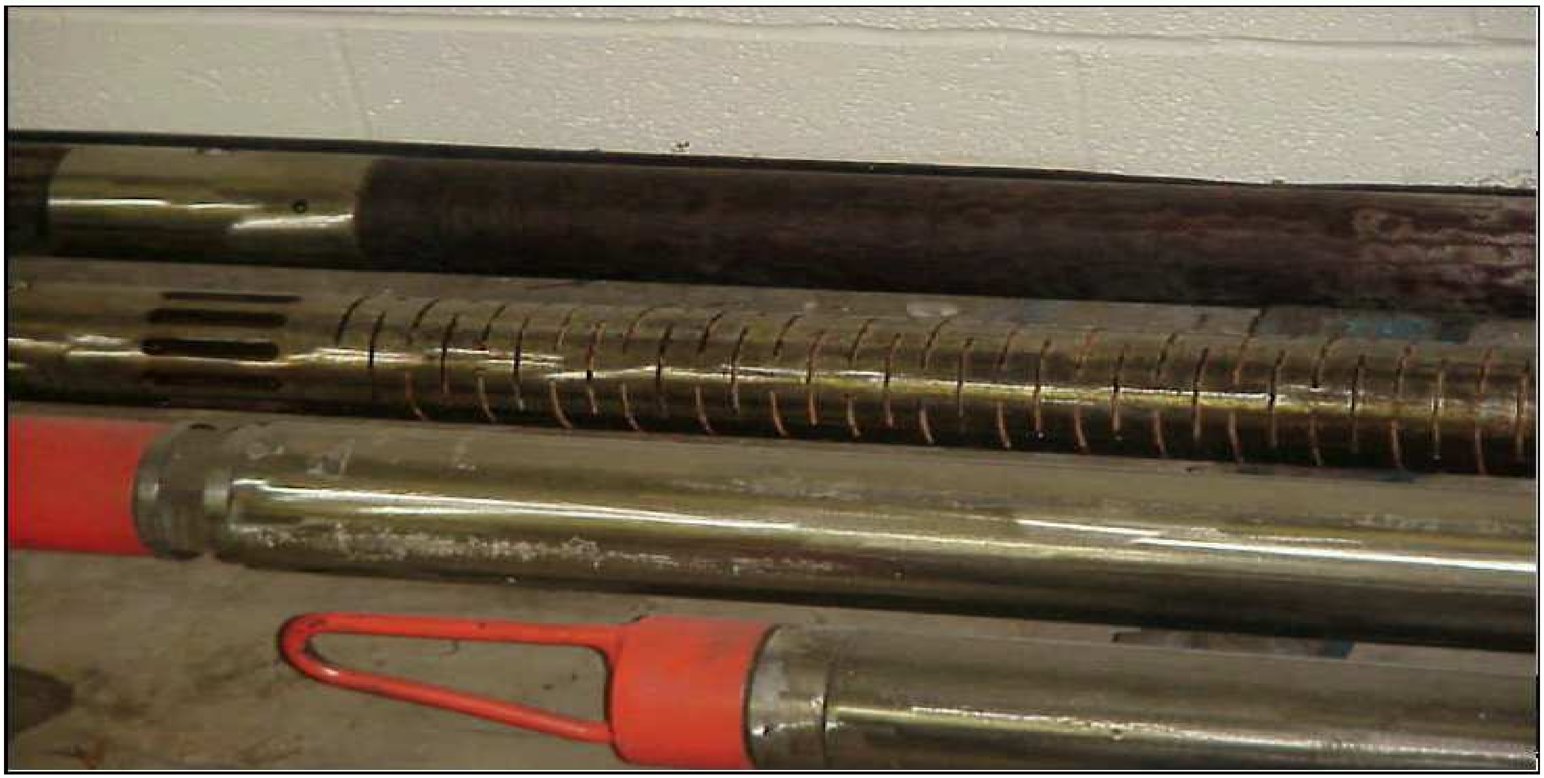

RESISTIVITY LOGGING INSTRUMENTS

Utility of Logging Instruments

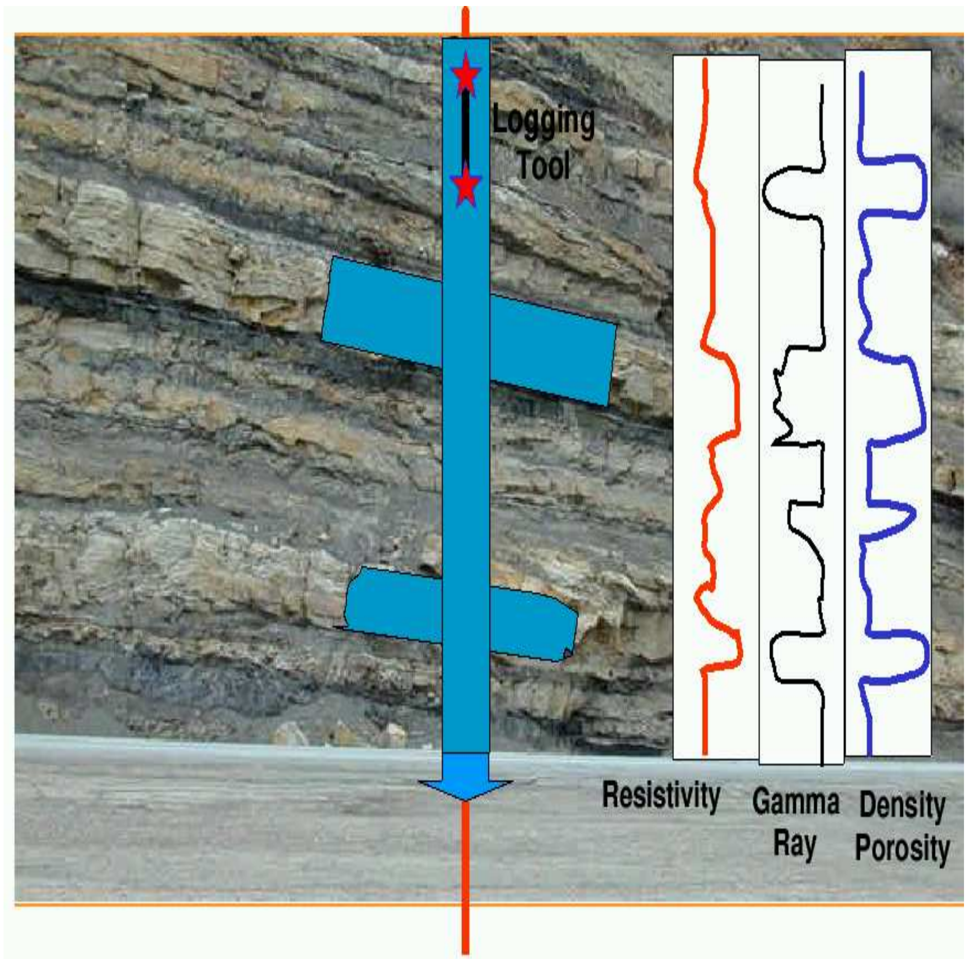

OBJECTIVES: To determine

- **Payzones (oil and gas).**
- **Amount of oil/gas.**
- **Ability to extract oil/gas.**

$

RESISTIVITY LOGGING INSTRUMENTS

Main Objective: To Solve an Inverse Problem

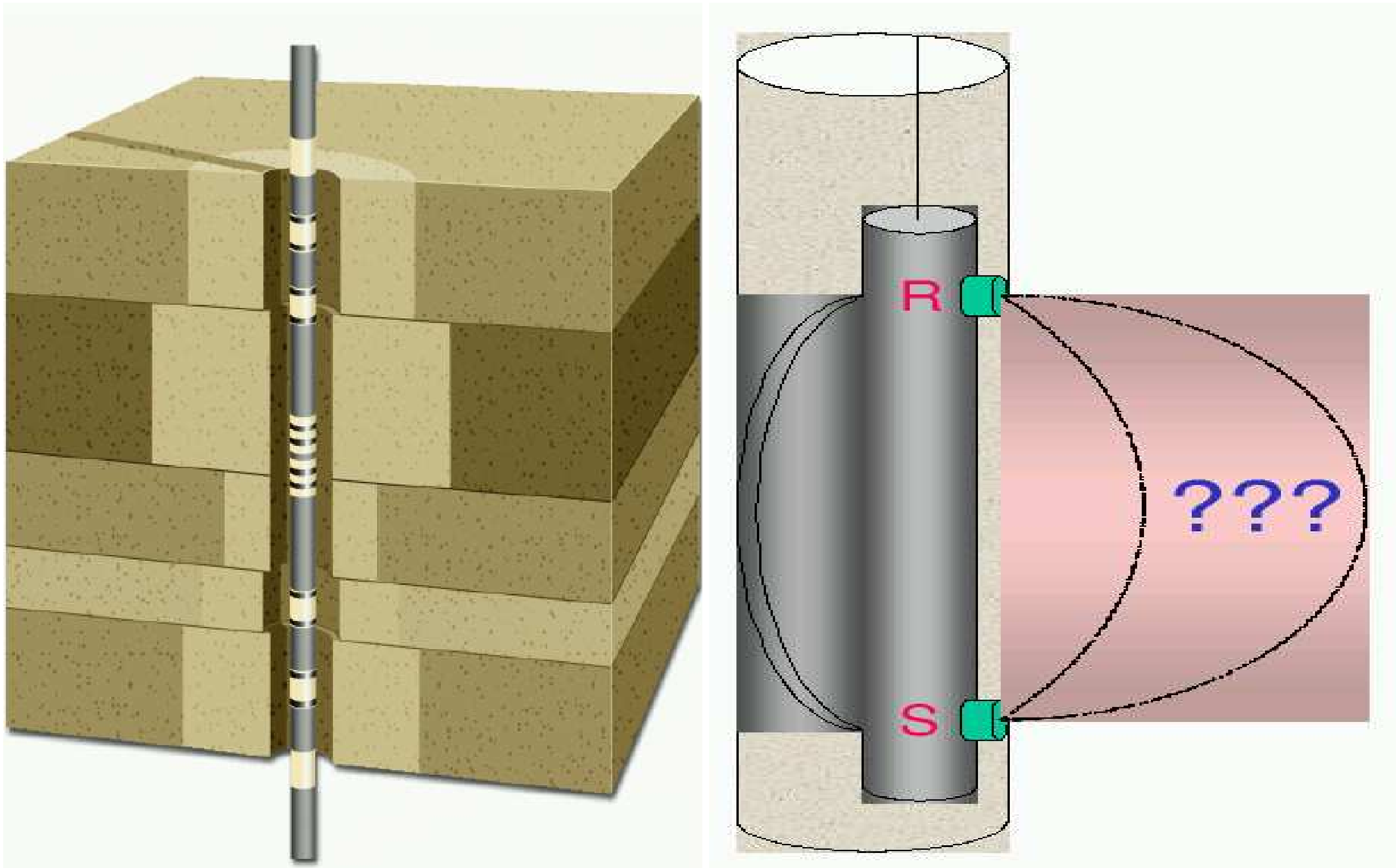

A software for solving the DIRECT problem is essential in order to solve the INVERSE problem

RESISTIVITY LOGGING INSTRUMENTS

Resistivity Logging Instruments

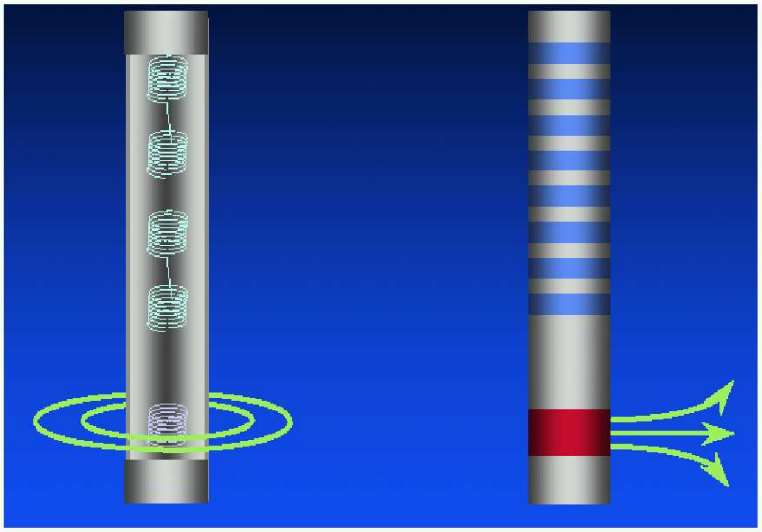

MAXWELL'S EQUATIONS

3D Variational Formulation

Time-Harmonic Maxwell's Equations

$\nabla \times \mathrm{H} = (\bar{\bar{\sigma}} + j\omega\bar{\bar{\epsilon}})\mathrm{E} + \mathrm{J}^{imp}$	**Ampere's law**
$\nabla \times \mathrm{E} = -j\omega\bar{\bar{\mu}}\mathrm{H} - \mathrm{M}^{imp}$	**Faraday's law**
$\nabla \cdot (\bar{\bar{\epsilon}}\mathrm{E}) = \rho$	**Gauss' law of Electricity**
$\nabla \cdot (\bar{\bar{\mu}}\mathrm{H}) = 0$	**Gauss' law of Magnetism**

E-VARIATIONAL FORMULATION:

$$\begin{cases} \text{Find } \mathrm{E} \in \mathrm{E}_D + \boldsymbol{H}_D(\mathrm{curl};\Omega) \text{ such that:} \\ \displaystyle\int_\Omega (\bar{\bar{\mu}}^{-1}\nabla \times \mathrm{E}) \cdot (\nabla \times \bar{\mathrm{F}})\, dV - \int_\Omega (\bar{\bar{k}}^2\mathrm{E}) \cdot \bar{\mathrm{F}}\, dV = -j\omega \int_\Omega \mathrm{J}^{imp} \cdot \bar{\mathrm{F}}\, dV \\ \displaystyle +j\omega \int_{\Gamma_N} \mathrm{J}^{imp}_{\Gamma_N} \cdot \bar{\mathrm{F}}_t\, dS - \int_\Omega (\bar{\bar{\mu}}^{-1}\mathrm{M}^{imp}) \cdot (\nabla \times \bar{\mathrm{F}})\, dV \quad \forall\, \mathrm{F} \in \boldsymbol{H}_D(\mathrm{curl};\Omega) \end{cases}$$

MAXWELL'S EQUATIONS

2D Variational Formulation (Axi-symmetric Problems)

E_ϕ -Variational Formulation (Azimuthal)

$$\left\{ \begin{array}{l} \textbf{Find } E_\phi \in E_{\phi,D} + \tilde{H}^1_D(\Omega) \textbf{ such that:} \\ \displaystyle\int_\Omega (\bar{\bar{\mu}}^{-1}_{\rho,z} \nabla \times \mathrm{E}_\phi) \cdot (\nabla \times \bar{\mathrm{F}}_\phi)\, dV - \int_\Omega (\bar{\bar{k}}^2_\phi \mathrm{E}_\phi) \cdot \bar{\mathrm{F}}_\phi \, dV = -j\omega \int_\Omega J^{imp}_\phi \, \bar{F}_\phi \, dV \\ \qquad \displaystyle + j\omega \int_{\Gamma_N} J^{imp}_{\phi,\Gamma_N} \, \bar{F}_\phi \, dS - \int_\Omega (\bar{\bar{\mu}}^{-1}_{\rho,z} \mathrm{M}^{imp}_{\rho,z}) \cdot \bar{\mathrm{F}}_\phi \, dV \qquad \forall\, F_\phi \in \tilde{H}^1_D(\Omega) \end{array} \right.$$

$\mathrm{E}_{\rho,z}$ -Variational Formulation (Meridian)

$$\left\{ \begin{array}{l} \textbf{Find } (E_\rho, E_z) \in \mathrm{E}_D + \tilde{H}_D(\mathrm{curl};\Omega) \textbf{ such that:} \\ \displaystyle\int_\Omega (\bar{\bar{\mu}}^{-1}_\phi \nabla \times \mathrm{E}_{\rho,z}) \cdot (\nabla \times \bar{\mathrm{F}}_{\rho,z})\, dV - \int_\Omega (\bar{\bar{k}}^2_{\rho,z} \mathrm{E}_{\rho,z}) \cdot \bar{\mathrm{F}}_{\rho,z}\, dV = \\ \qquad \displaystyle -j\omega \int_\Omega J^{imp}_\rho \bar{F}_\rho + J^{imp}_z \bar{F}_z \, dV + j\omega \int_{\Gamma_N} J^{imp}_{\rho,\Gamma_N} \bar{F}_\rho + J^{imp}_{z,\Gamma_N} \bar{F}_z \, dS \\ \qquad \displaystyle - \int_\Omega (\bar{\bar{\mu}}^{-1}_\phi \mathrm{M}^{imp}_\phi) \cdot \bar{\mathrm{F}}_{\rho,z}\, dV \qquad \forall\, (F_\rho, F_z) \in \tilde{H}_D(\mathrm{curl};\Omega) \end{array} \right.$$

MODEL PROBLEMS OF INTEREST

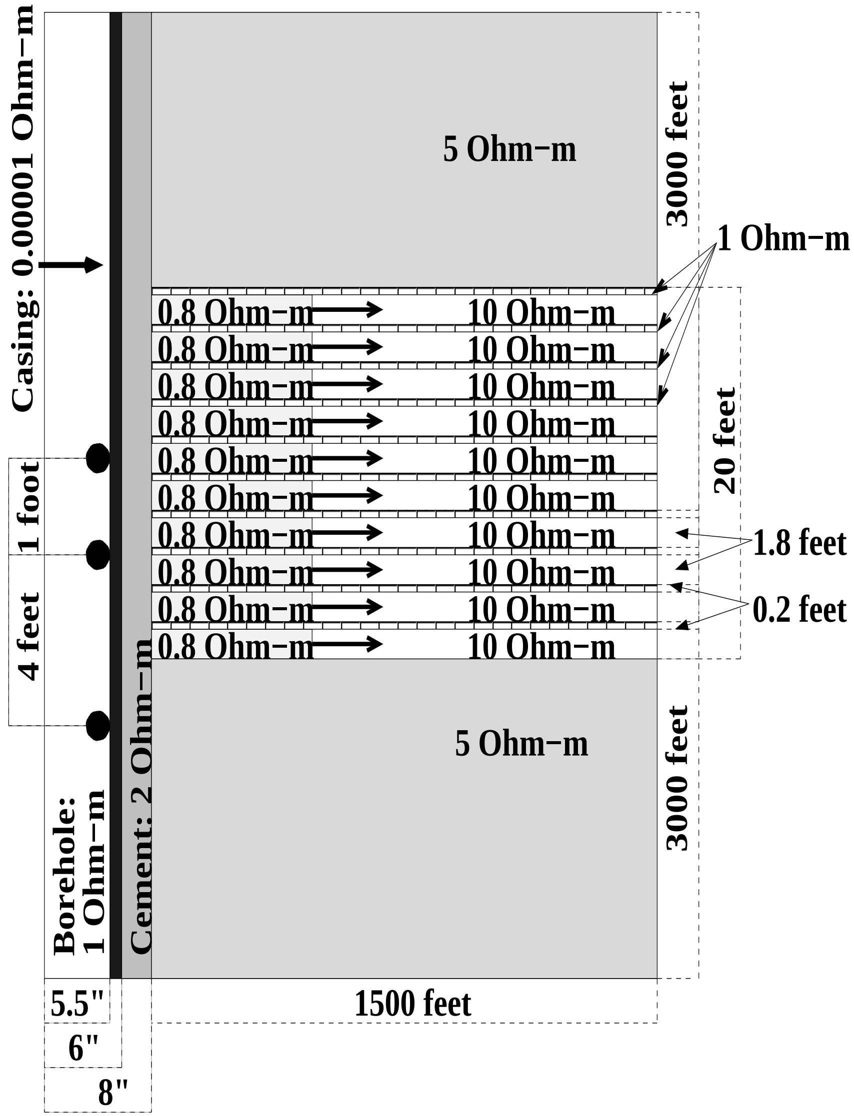

Axisymmetric 3D problem.

Seven different materials.

Through casing resistivity instrument.

Large variations on resistivity.

Objective: Study the effect of invasion THROUGH CASING on laminated sands.

MODEL PROBLEMS OF INTEREST

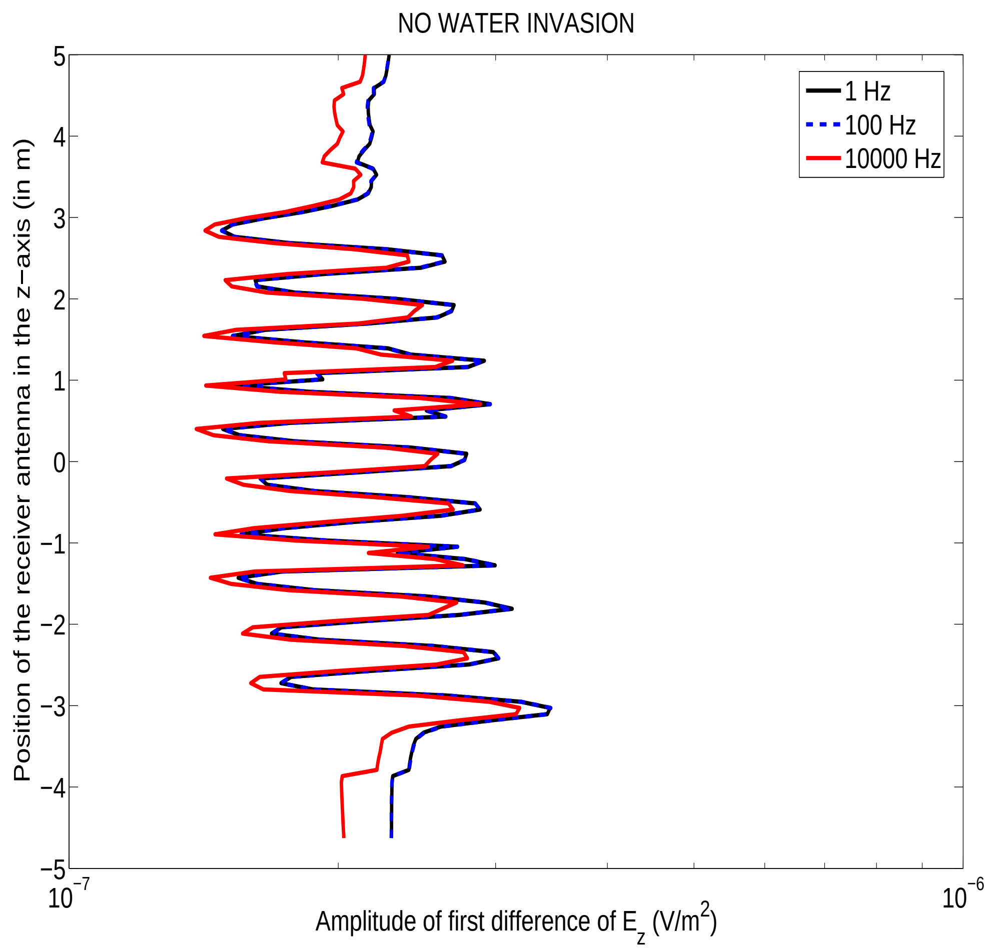

Variations due to frequency are small (below 5%)

THE hp-FINITE ELEMENT METHOD (FEM)

The h-Finite Element Method

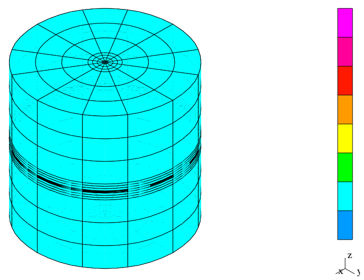

1. Convergence limited by the polynomial degree, and large material contrasts.
2. Optimal *h*-grids do NOT converge exponentially in real applications.
3. They may “lock” (100$\%$ error).

The p-Finite Element Method

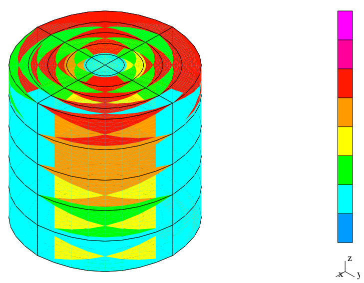

1. Exponential convergence feasible for analytical (“nice”) solutions.
2. Optimal *p*-grids do NOT converge exponentially in real applications.
3. If initial *h*-grid is not adequate, the *p*-method will fail miserably.

The hp-Finite Element Method

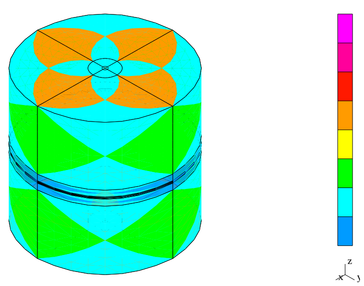

1. Exponential convergence feasible for ALL solutions.
2. Optimal *hp*-grids DO converge exponentially in real applications.
3. If initial *hp*-grid is not adequate, results will still be great.

GOAL-ORIENTED ADAPTIVITY

Mathematical Formulation (Goal-Oriented Adaptivity)

Let's L be the quantity of interest (Ex.: first vertical difference of electric field).

We consider the following problem (in variational form):

$$\begin{cases} \text{Find } L(\Psi)\text{, where } \Psi \in V \text{ such that :} \\ b(\Psi, \xi) = f(\xi) \quad \forall \xi \in V \ . \end{cases}$$

We define residual $r_e(\xi) = b(e, \xi)$. We seek for solution G of:

$$\begin{cases} \text{Find } G \in V'' \sim V \text{ such that :} \\ G(r_e) = L(e) \ . \end{cases}$$

This is necessarily solved if we find the solution of the *dual* problem:

$$\begin{cases} \text{Find } G \in V \text{ such that :} \\ b(\Psi, G) = L(\Psi) \quad \forall \Psi \in V \ . \end{cases}$$

Notice that $L(e) = b(e, G)$.

GOAL-ORIENTED ADAPTIVITY

Mathematical Formulation (Goal-Oriented Adaptivity)

DIRECT PROBLEM - Ψ -
2D Cross-Section

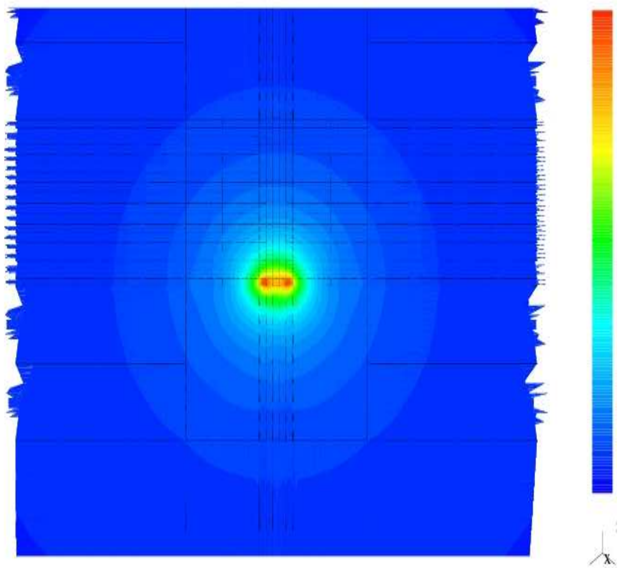

DUAL PROBLEM - G -
2D Cross-Section

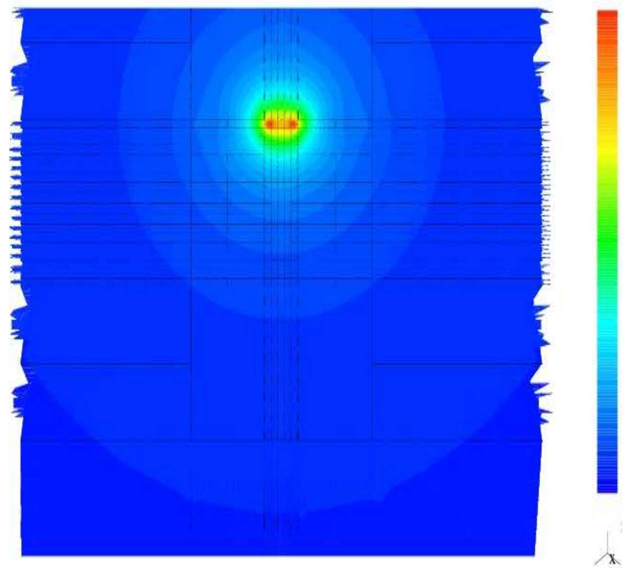

Representation Formula for the Error in the Quantity of Interest:

$$L(\Psi)=b(\Psi,G) = \int_\Omega \sigma \nabla\Psi \nabla G dV$$

GOAL-ORIENTED ADAPTIVITY

Mathematical Formulation (Goal-Oriented Adaptivity)

We define: $e = \Psi - \Psi_{hp}$, Ψ **exact solution of direct problem**

$\epsilon = G - G_{hp}$. G **exact solution of dual problem**

Upper Bound for the Error in the Quantity of Interest:

$$|L(e)| = |b(e,G)| = |b(e,\epsilon)| = |\int_\Omega \sigma \, \nabla e \, \nabla \epsilon \, dV| \leq$$

ALGORITHM I: $\sum_K |\int_K \sigma \, \nabla e \, \nabla \epsilon \, dV| \leq$

ALGORITHM II: $\sum_K \sqrt{\int_K \sigma \, (\nabla e)^2 \, dV} \sqrt{\int_K \sigma \, (\nabla \epsilon)^2 \, dV}$

SELF-ADAPTIVE GOAL-ORIENTED hp-FEM

Algorithm for Goal-Oriented Adaptivity - STEP I -

Solve Direct and Dual Problems on Grid hp

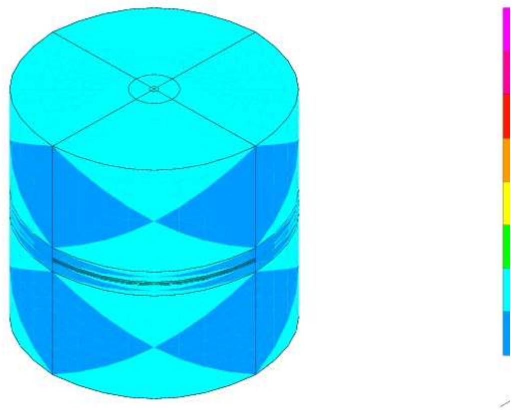

$\longrightarrow$

Solve Direct and Dual Problems on Grid $h/2, p+1$

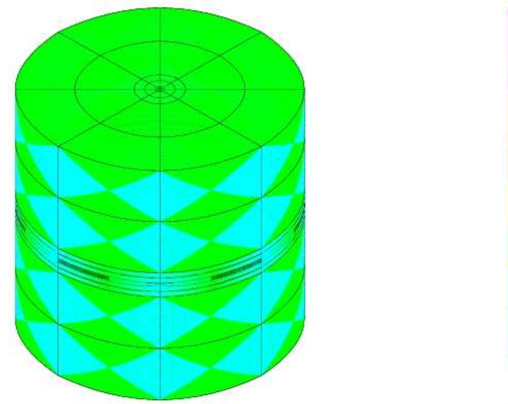

Use the fine grid solution to estimate the coarse grid error function.
Apply the fully automatic goal-oriented hp-adaptive algorithm.

Next optimal hp-grid:

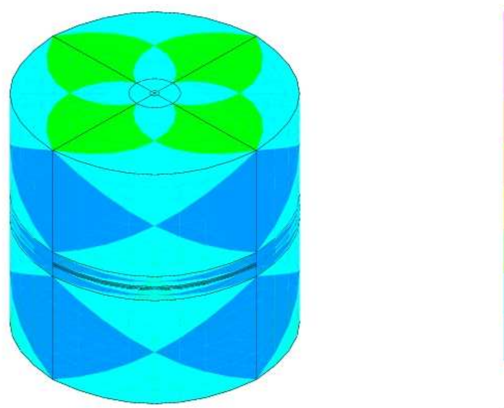

SELF-ADAPTIVE GOAL-ORIENTED hp-FEM

Algorithm for Goal-Oriented Adaptivity - STEP II -

Solve Direct and Dual Problems on Grid hp

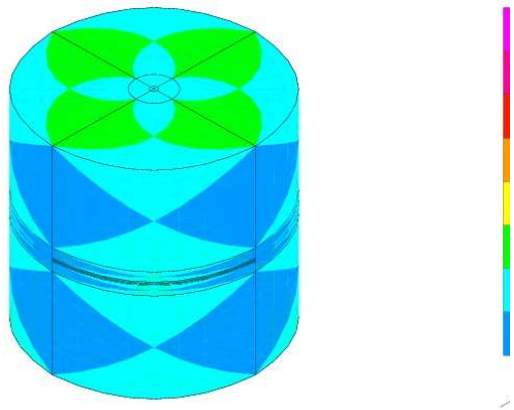

$\longrightarrow$

Solve Direct and Dual Problems on Grid $h/2, p+1$

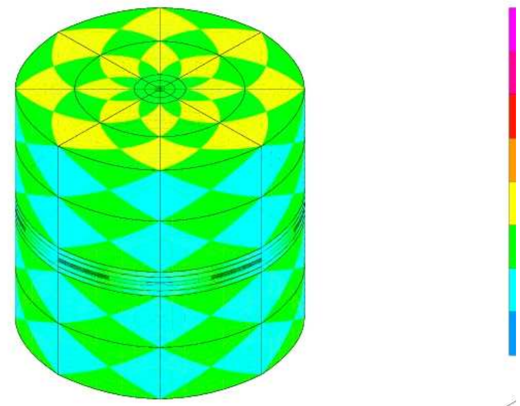

Use the fine grid solution to estimate the coarse grid error function. Apply the fully automatic goal-oriented hp-adaptive algorithm.

Next optimal hp-grid:

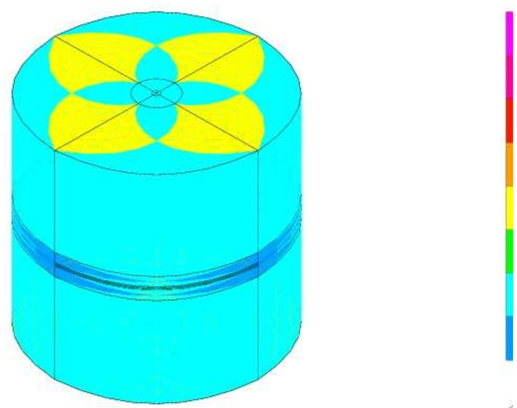

SELF-ADAPTIVE GOAL-ORIENTED hp-FEM

Algorithm for Goal-Oriented Adaptivity - STEP III -

Solve Direct and Dual Problems on Grid hp

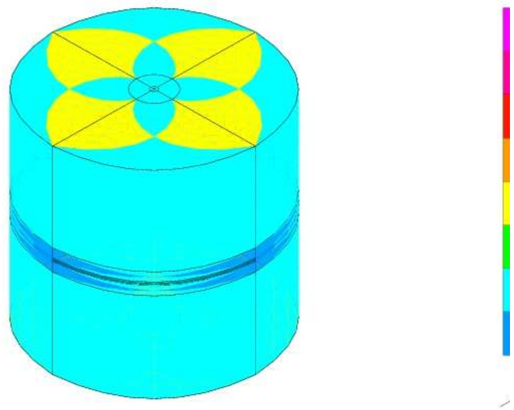

$\longrightarrow$

Solve Direct and Dual Problems on Grid $h/2, p+1$

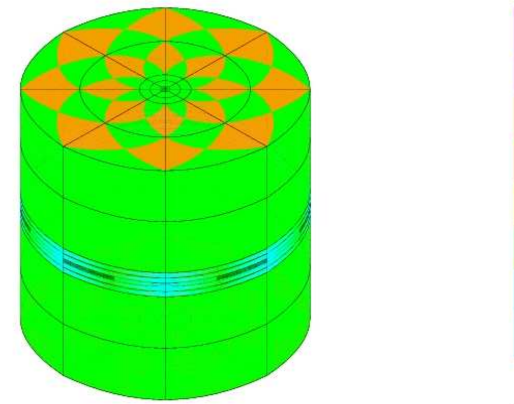

Use the fine grid solution to estimate the coarse grid error function.
Apply the fully automatic goal-oriented hp-adaptive algorithm.

Next optimal hp-grid:

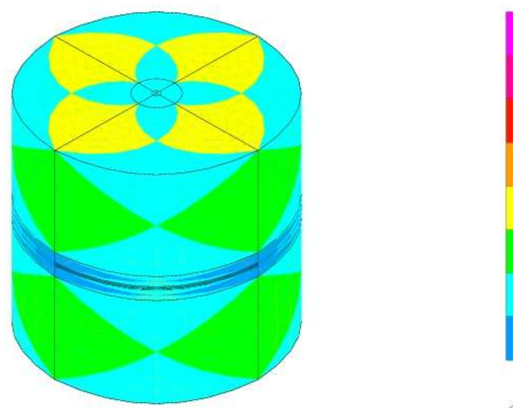

SELF-ADAPTIVE GOAL-ORIENTED hp-FEM

Algorithm for Goal-Oriented Adaptivity - STEP IV -

Solve Direct and Dual Problems on Grid hp

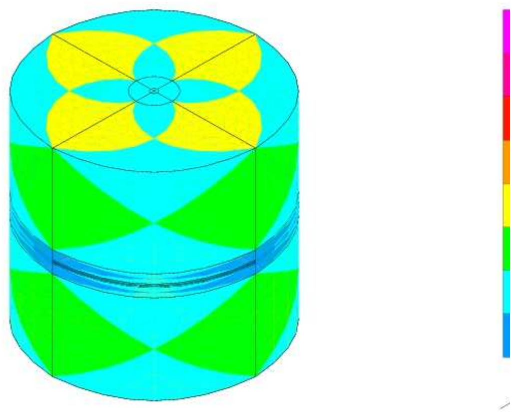

$\longrightarrow$

Solve Direct and Dual Problems on Grid $h/2, p+1$

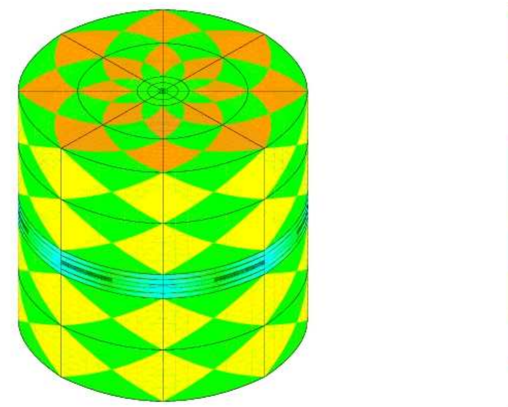

Use the fine grid solution to estimate the coarse grid error function.
Apply the fully automatic goal-oriented hp-adaptive algorithm.

Next optimal hp-grid:

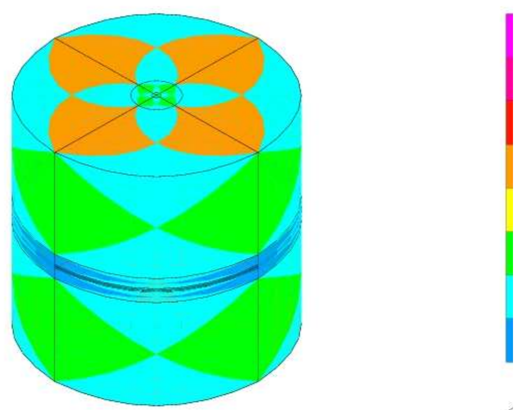

2D hp-FEM: NUMERICAL RESULTS

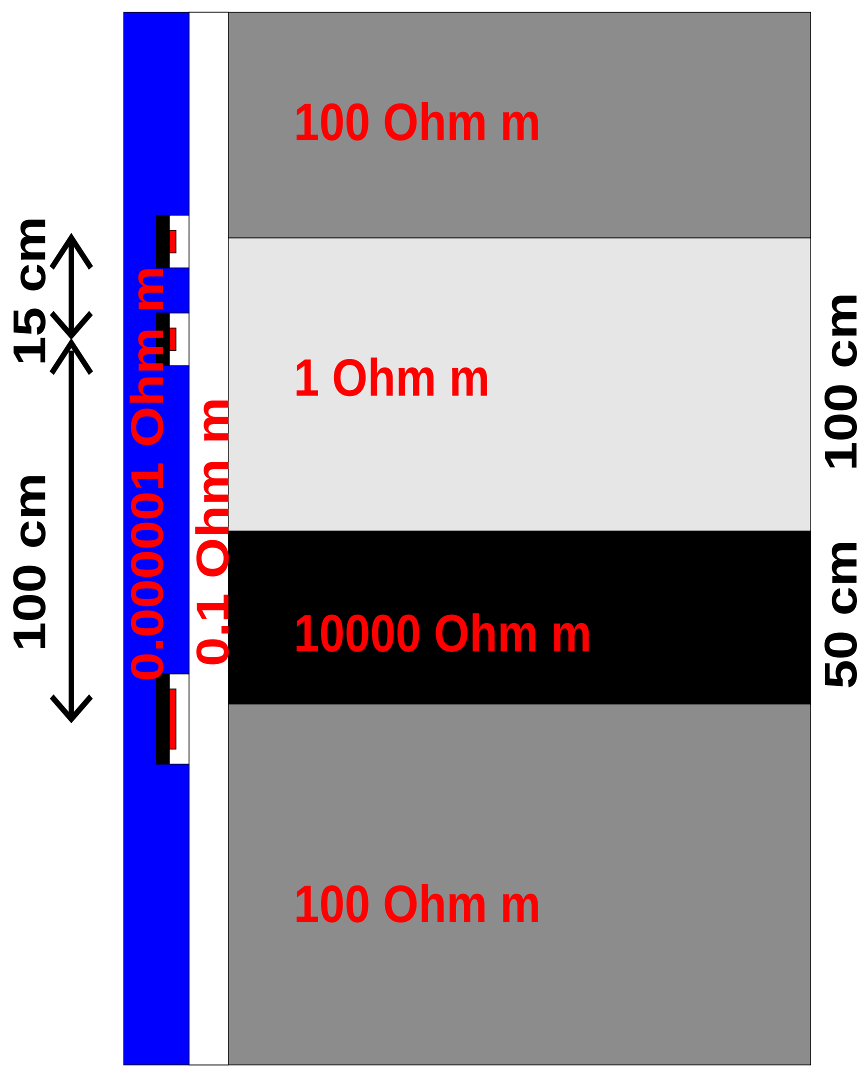

Description of Antennas

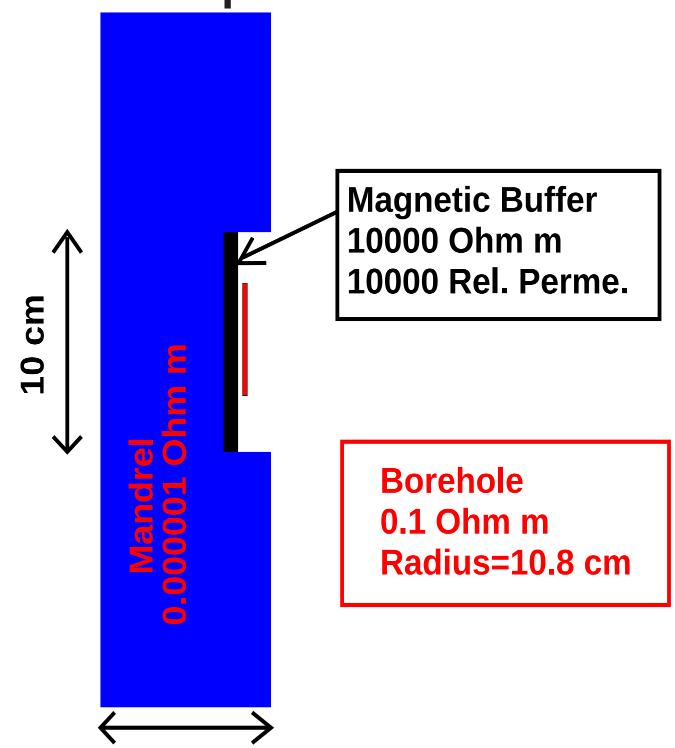

Goal: To Study the Effect of Invasion, Anistotropy, and Magnetic Permeability.

2D hp-FEM: NUMERICAL RESULTS

First. Vert. Diff. E_ϕ (solenoid). Position: 0.475m

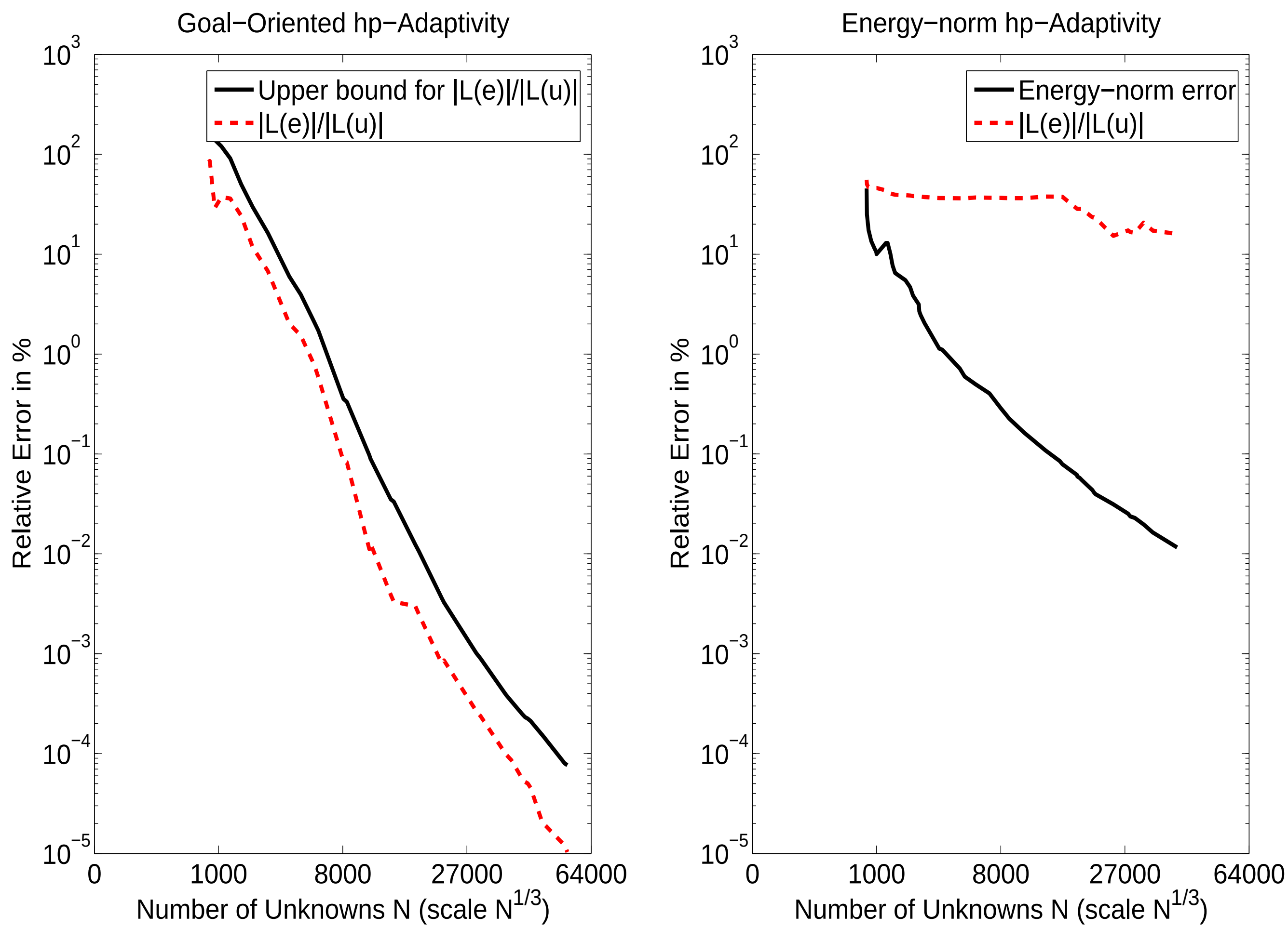

2D hp-FEM: NUMERICAL RESULTS

Goal-Oriented vs. Energy-norm hp-Adaptivity

Problem with Mandrel at 2 Mhz.

Continuous Elements (Goal-Oriented Adaptivity)

Quantity of Interest	Real Part	Imag Part
COARSE GRID	-0.1629862203E-01	-0.4016944732E-02
FINE GRID	-0.1629862347E-01	-0.4016944223E-02

Continuous Elements (Energy-norm Adaptivity)

Quantity of Interest	Real Part	Imag Part
0.01% ENERGY ERROR	-0.1382759158E-01	-0.2989492851E-02

It is critical to use GOAL-ORIENTED adaptivity.

2D hp-FEM: NUMERICAL RESULTS

First. Vert. Diff. E_ϕ (solenoid). Position: 0.475m

GOAL-ORIENTED HP-ADAPTIVITY (Quadrilateral Elements)

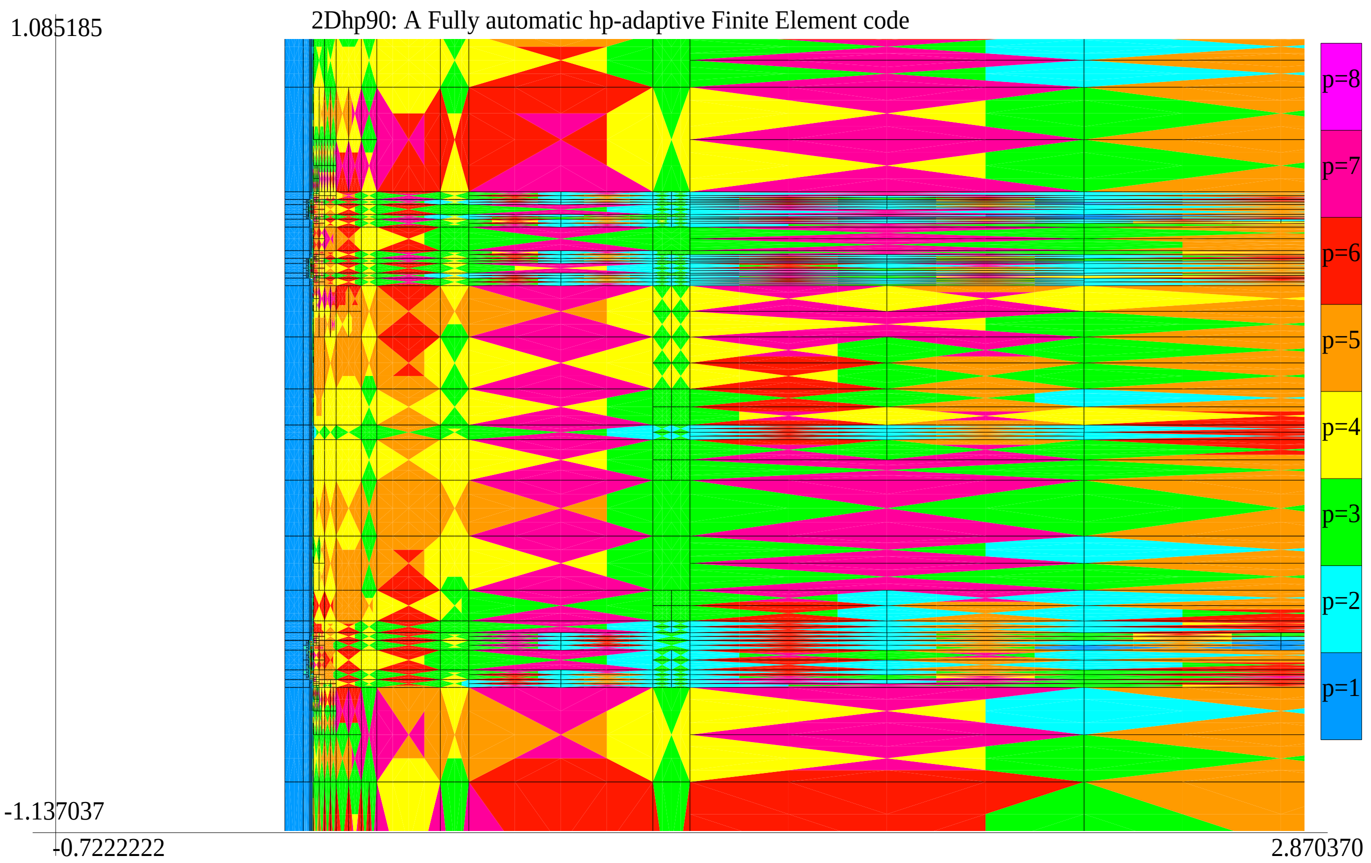

2D hp-FEM: NUMERICAL RESULTS

First. Vert. Diff. E_ϕ (solenoid). Position: 0.475m

GOAL-ORIENTED HP-ADAPTIVITY (ZOOM TOWARDS FIRST RECEIVER ANTENNA)

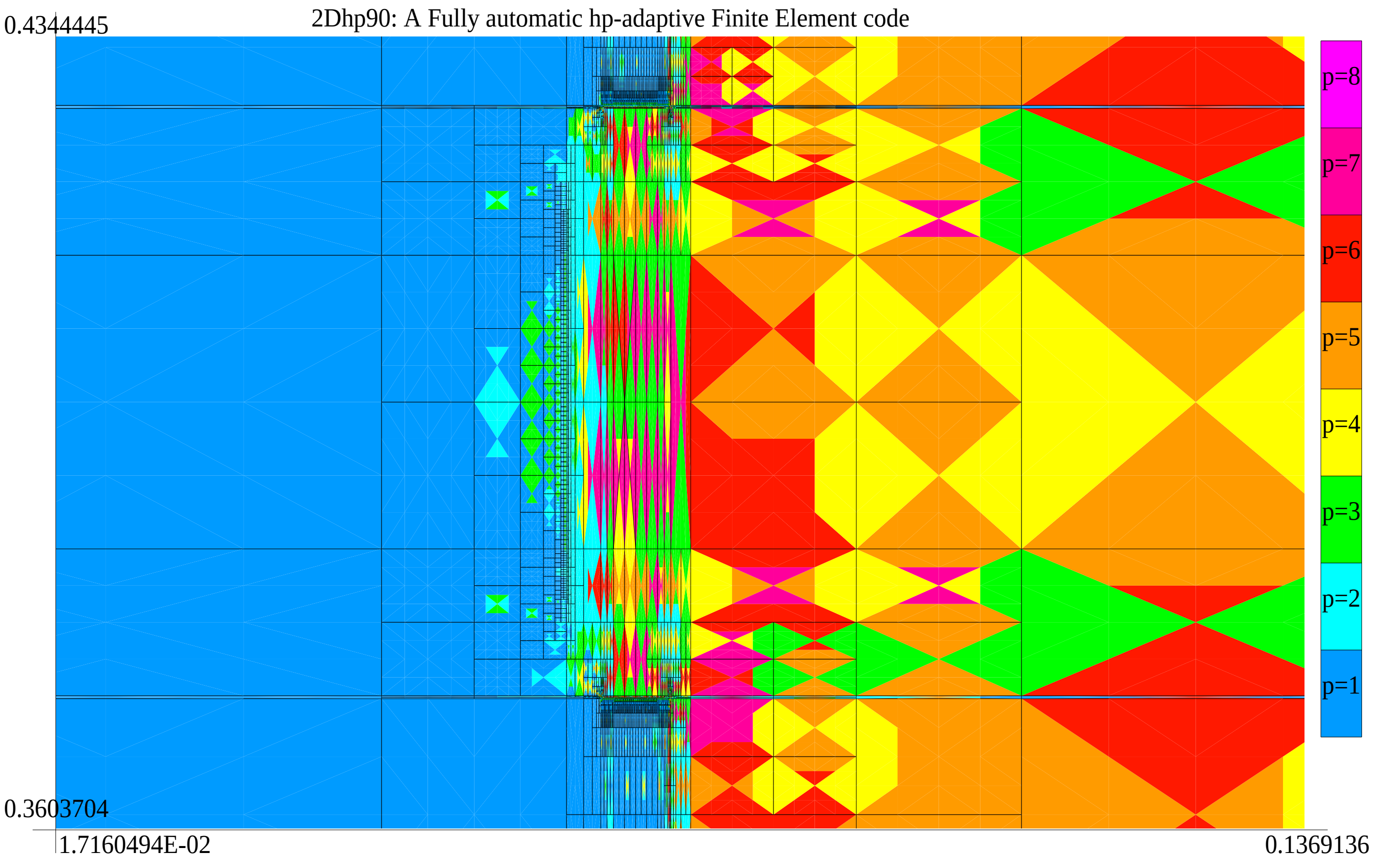

2D hp-FEM: NUMERICAL RESULTS

First Vert. Diff. H_ϕ for different antennas

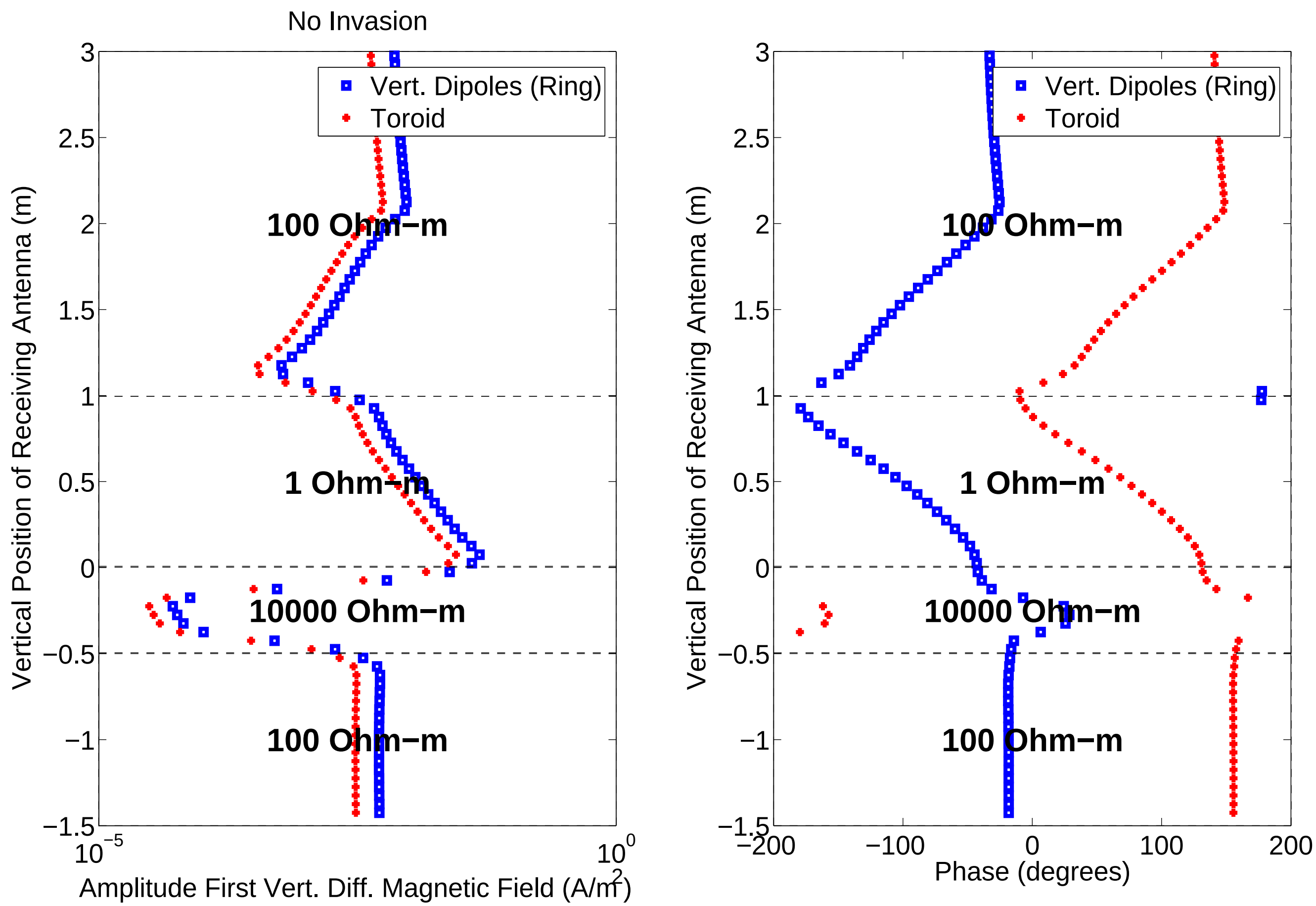

In LWD instruments, we obtain similar results using toroids or a ring of vert. dipoles

2D hp-FEM: NUMERICAL RESULTS

First Vert. Diff. E_z for a toroid antenna

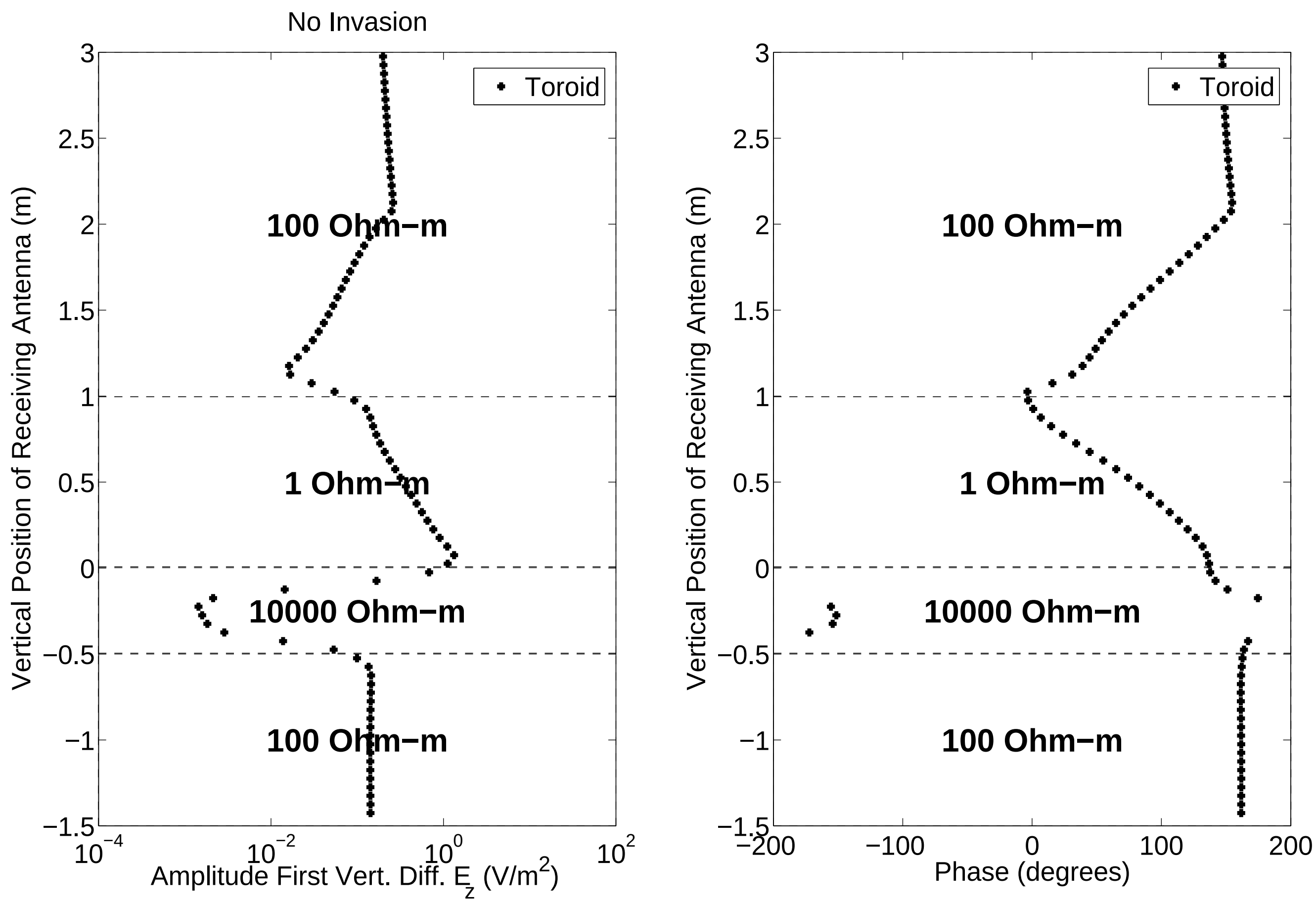

Toroids are adequate for identifying highly resistive layers

2D hp-FEM: NUMERICAL RESULTS

First Vert. Diff. E_ϕ for a solenoid antenna

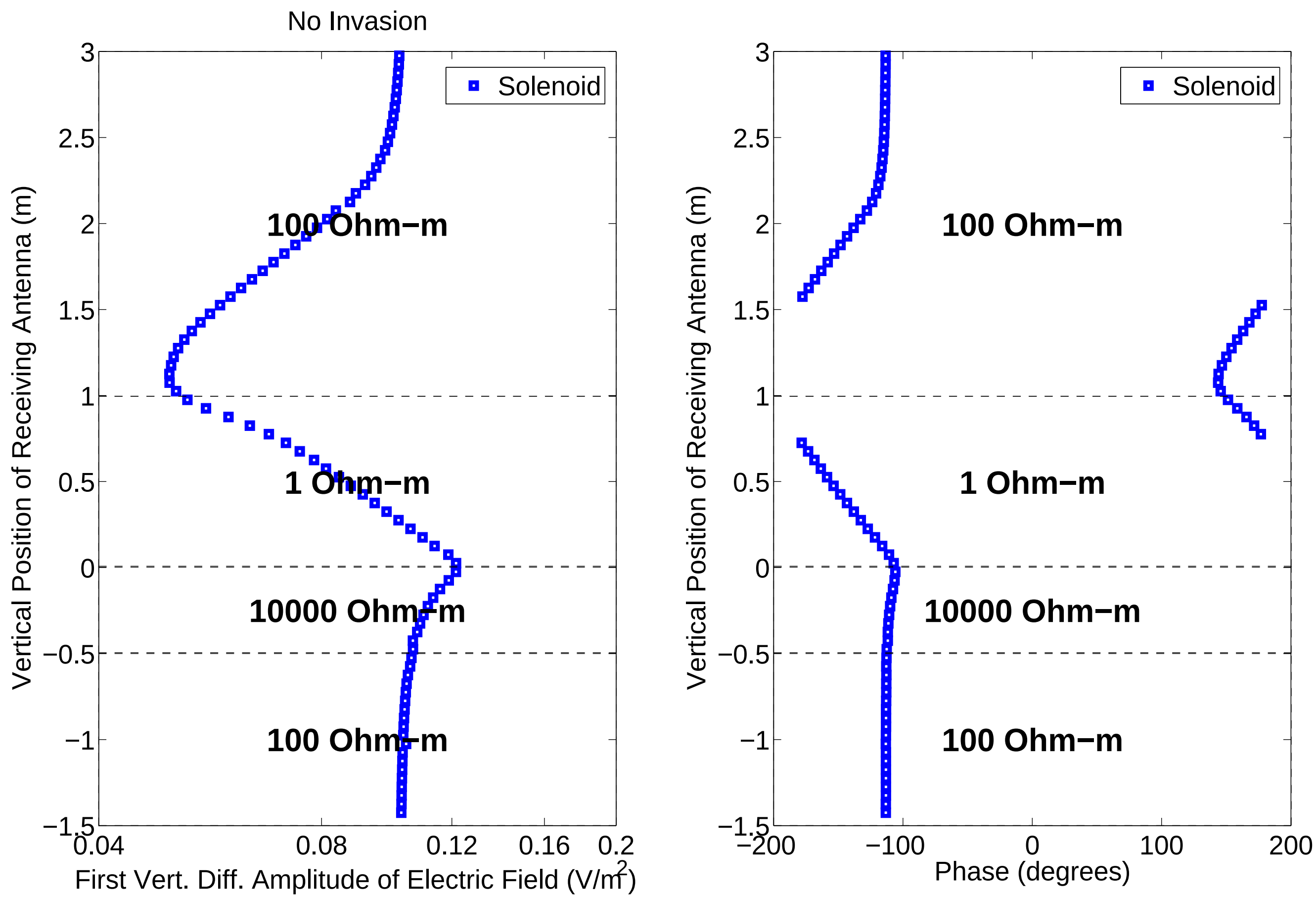

Solenoids are adequate for identifying low resistive layers

2D hp-FEM: NUMERICAL RESULTS

Use of Magnetic Buffers (E_ϕ for a solenoid)

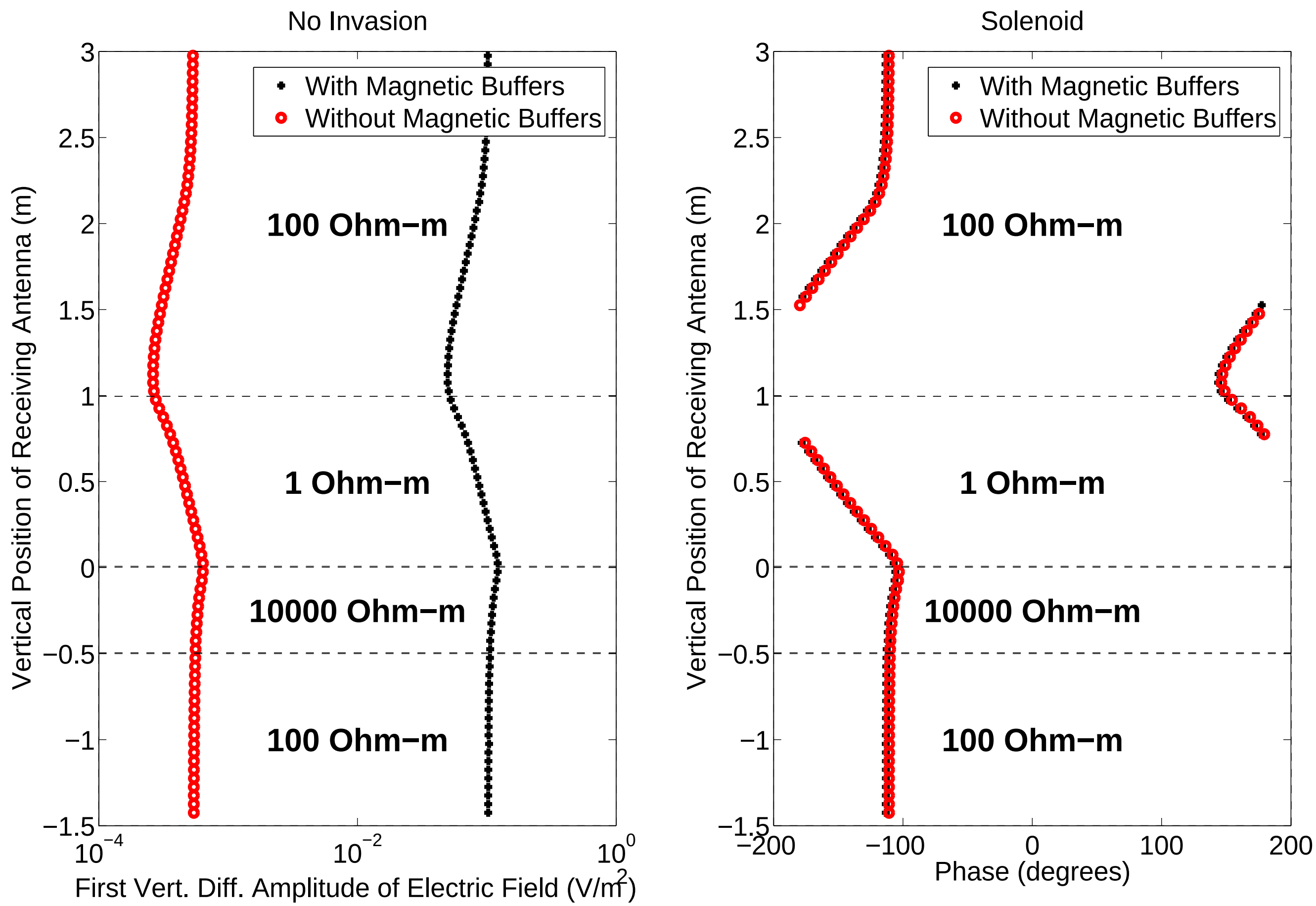

Use of magnetic buffers strengthen the signal in combination with solenoids

2D hp-FEM: NUMERICAL RESULTS

Use of Magnetic Buffers (H_ϕ for a toroid)

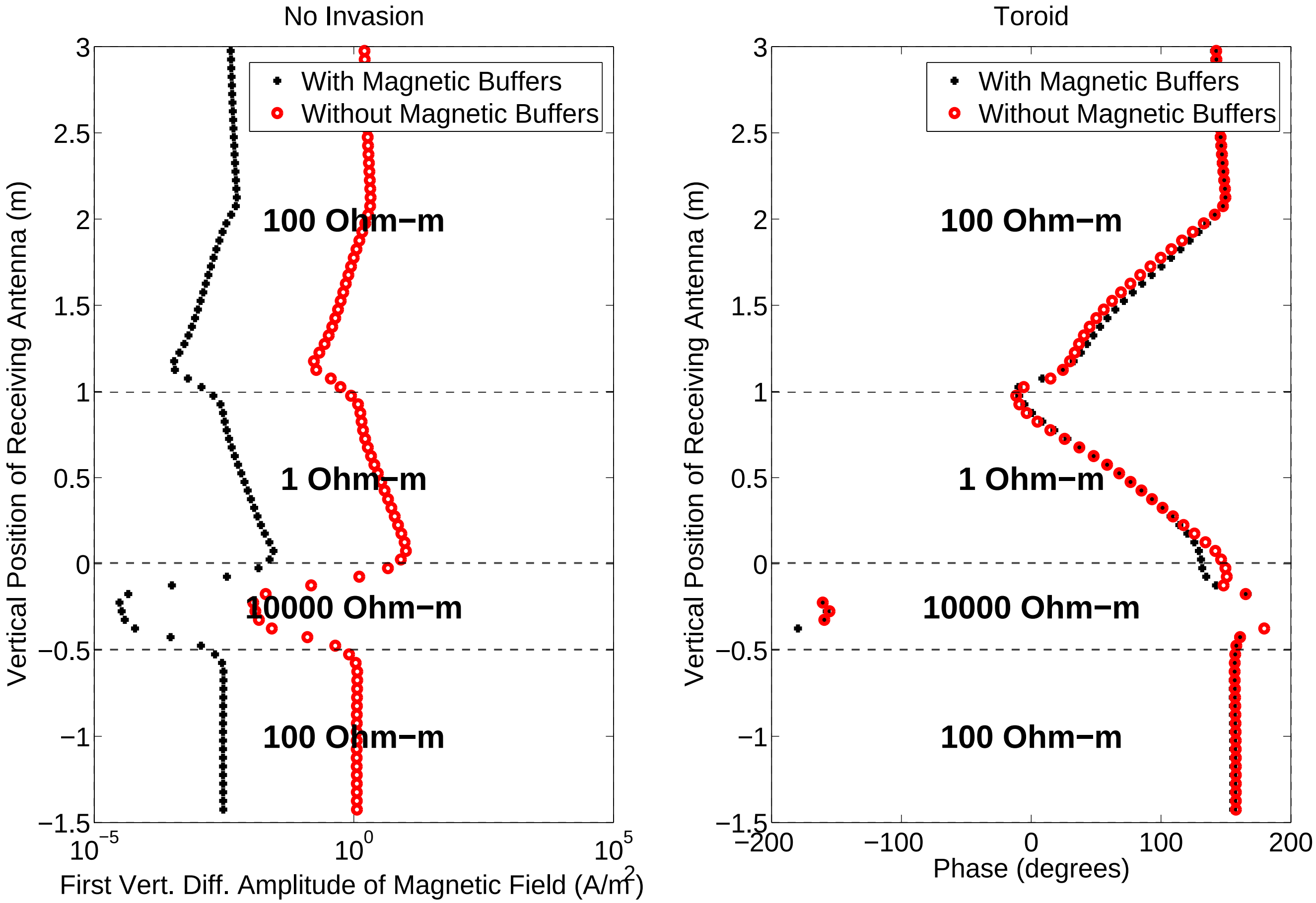

However, magnetic buffers weaken the signal in combination with toroids

2D hp-FEM: NUMERICAL RESULTS

Invasion study (E_ϕ for a solenoid)

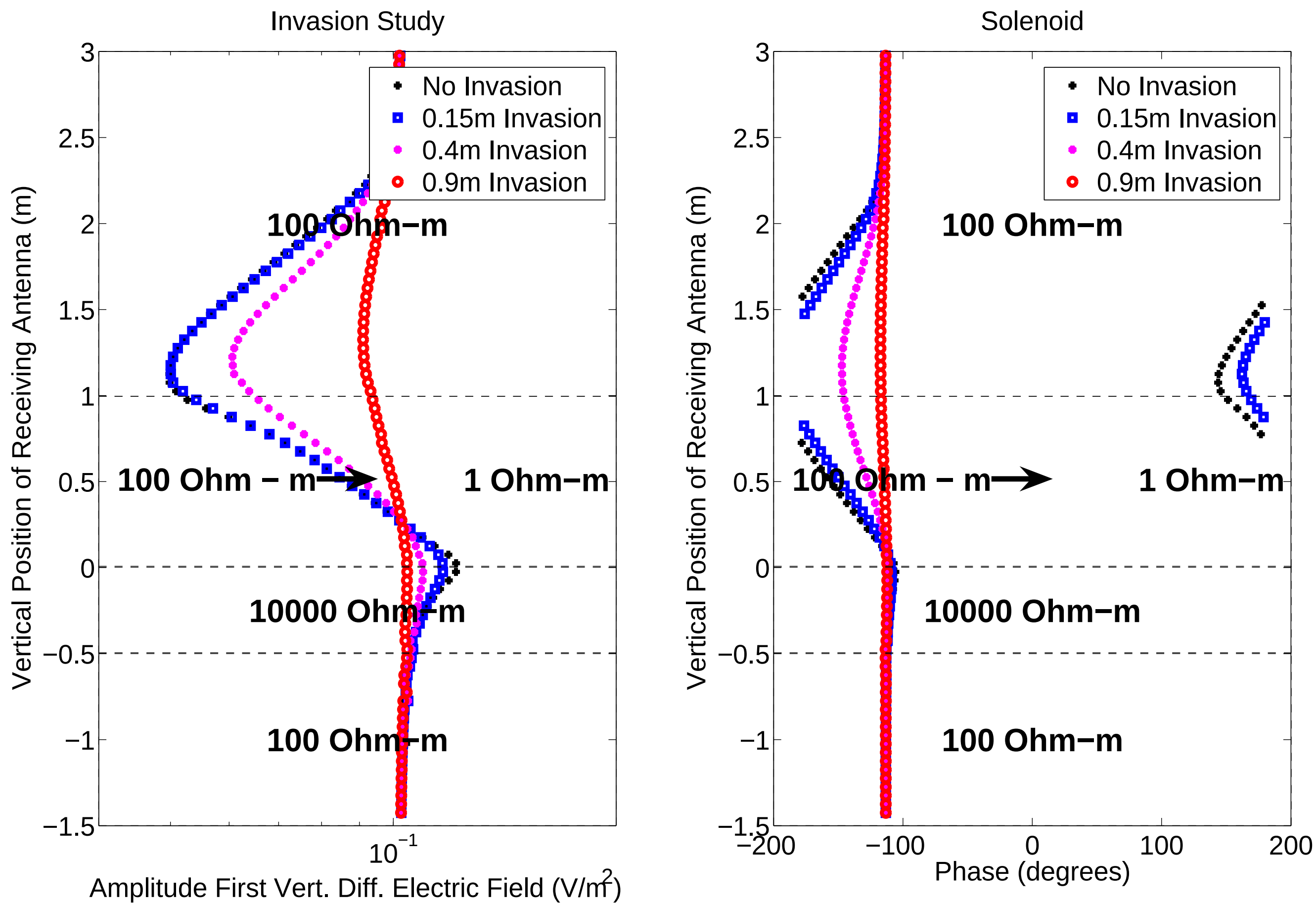

Large invasion effects can be sensed using solenoids

2D hp-FEM: NUMERICAL RESULTS

Invasion study (H_ϕ for a toroid)

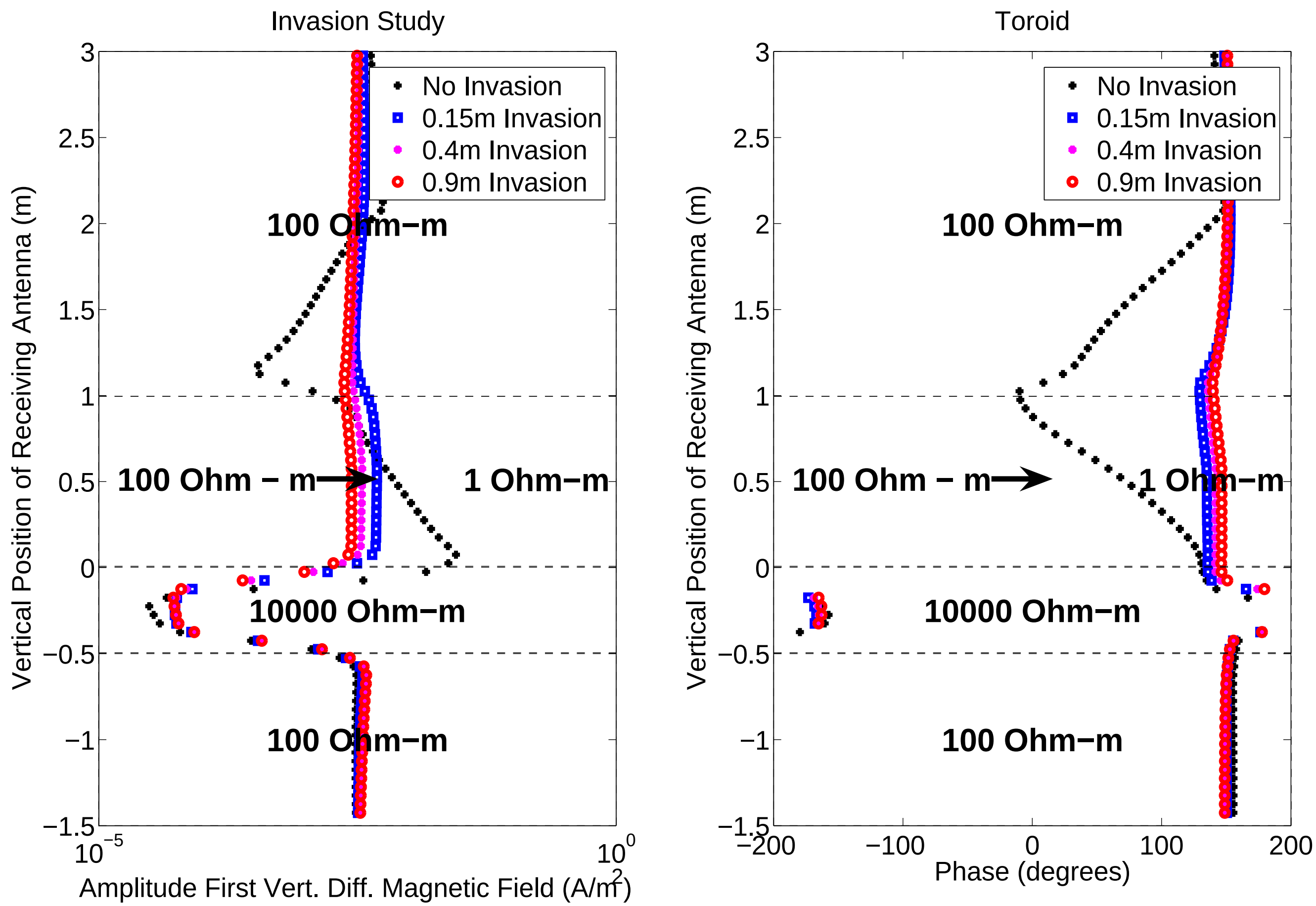

Small invasion effects can be sensed using toroids

2D hp-FEM: NUMERICAL RESULTS

Invasion study (E_ϕ for a solenoid)

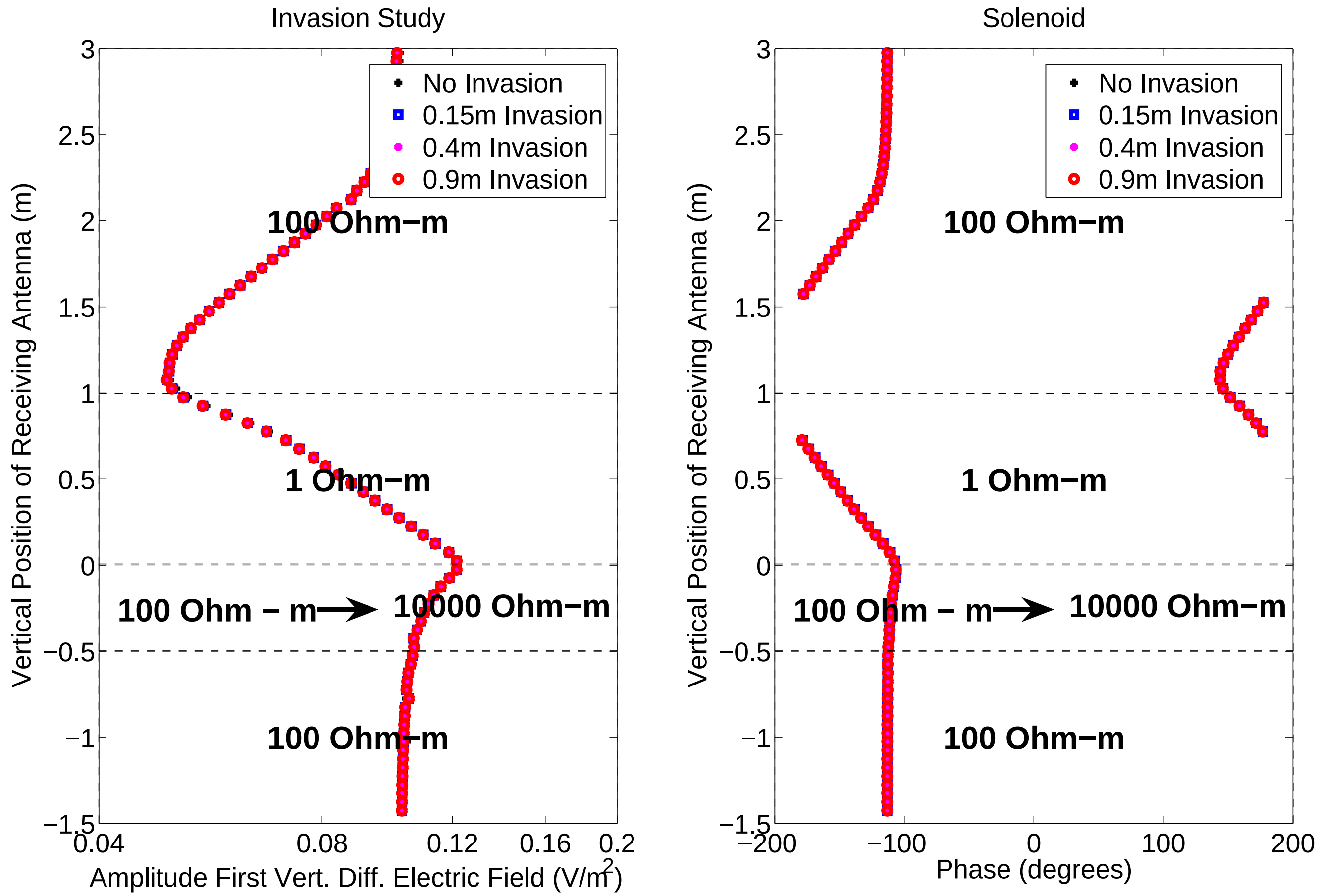

Invasion in resistive layers cannot be sensed using solenoids

2D hp-FEM: NUMERICAL RESULTS

Invasion study (H_ϕ for a toroid)

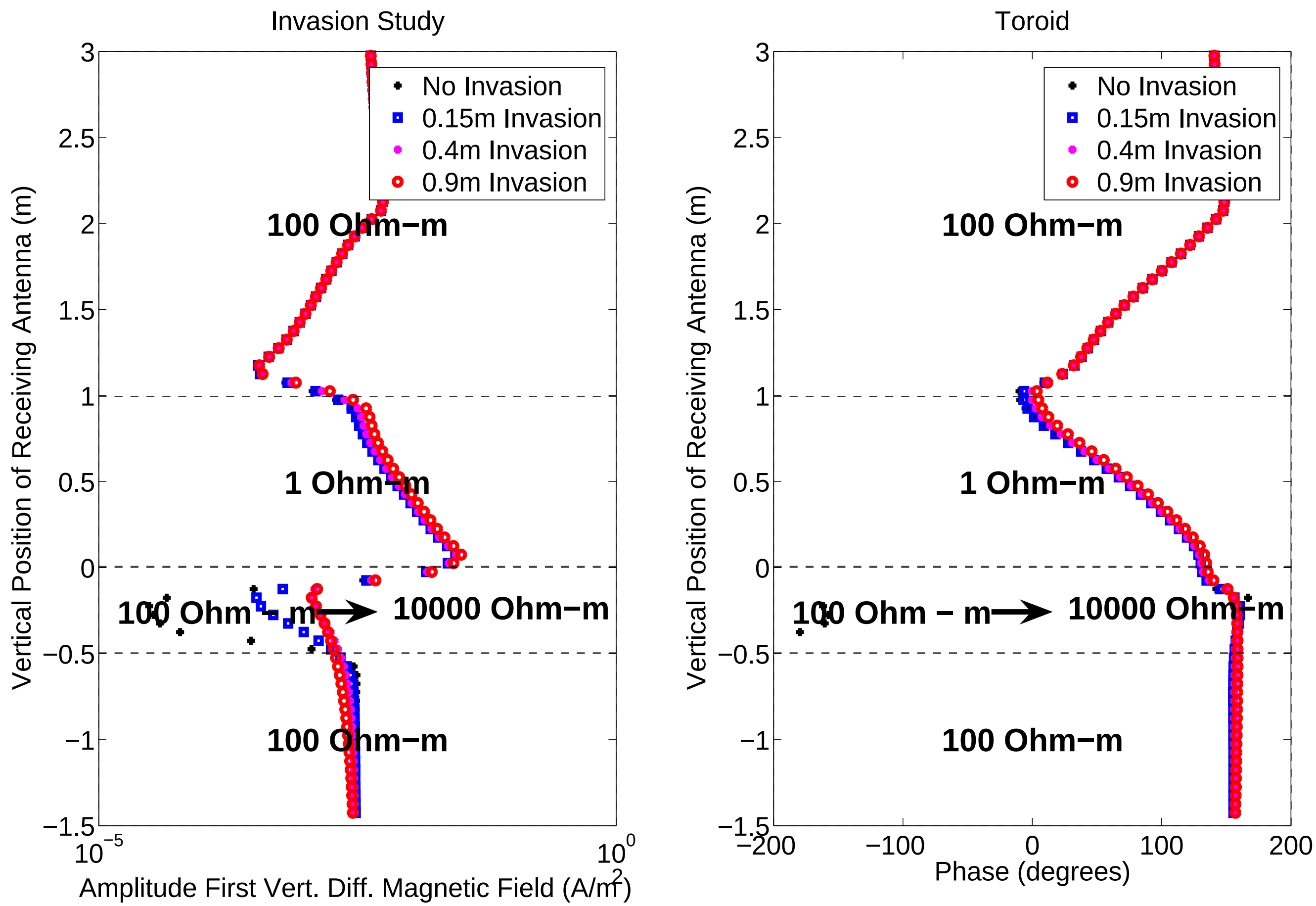

Invasion in resistive layers should be studied using toroids

2D hp-FEM: NUMERICAL RESULTS

Invasion and mandrel magnetic permeab. (E_ϕ)

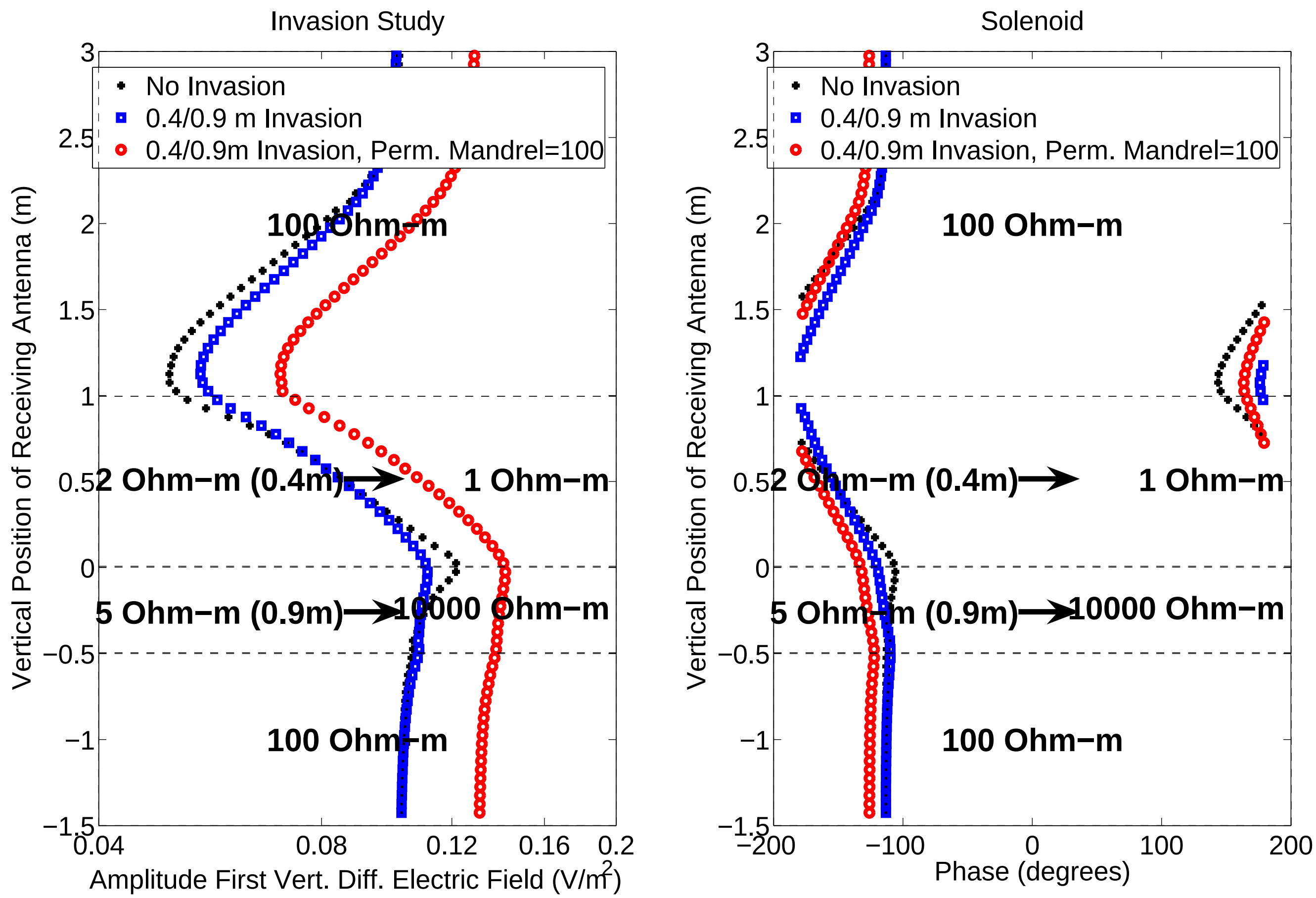

The effect of magnetic permeability on the mandrel is similar to the effect of magnetic buffers

2D hp-FEM: NUMERICAL RESULTS

Anisotropy (H_ϕ)

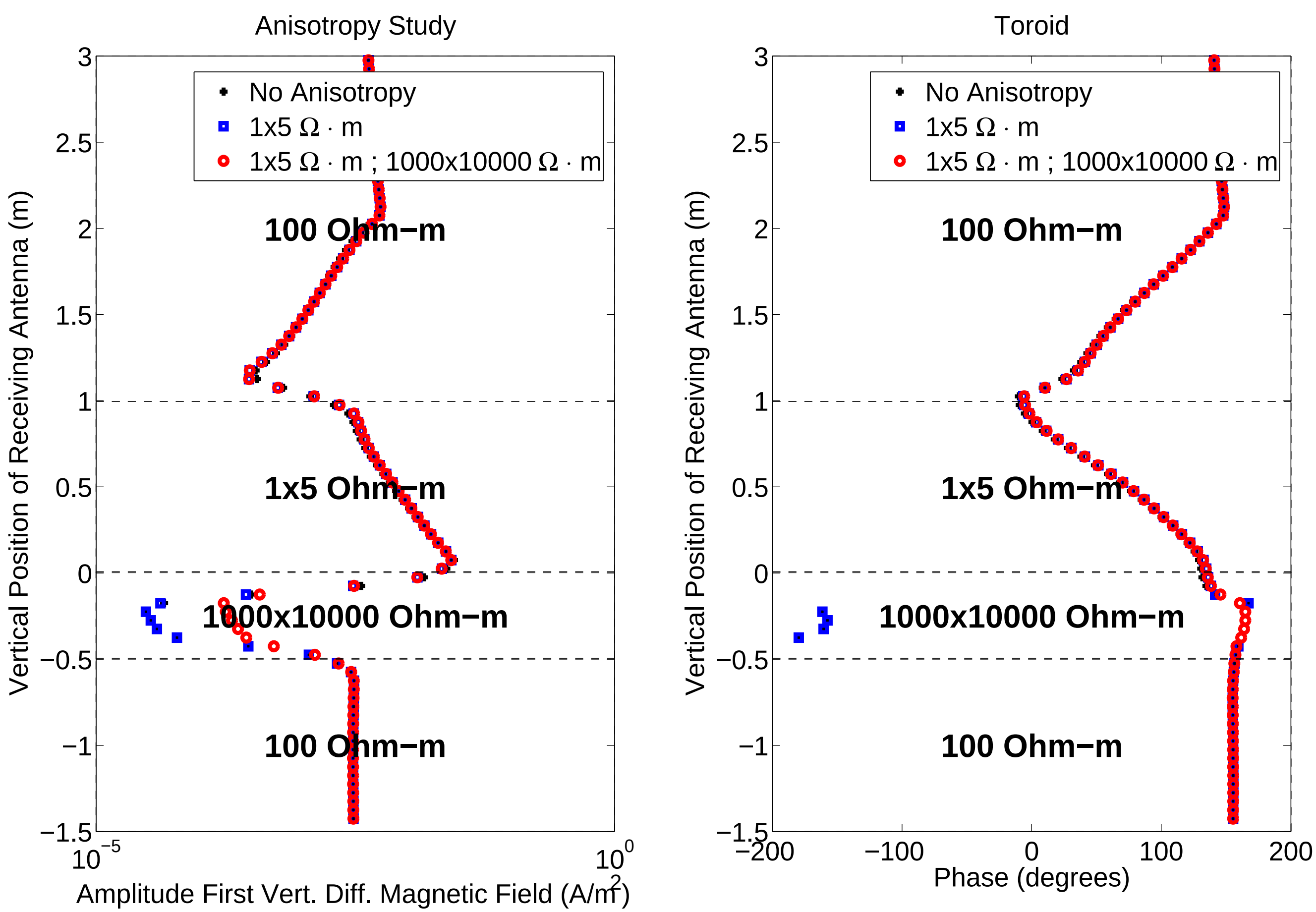

Anisotropy effects may be important when studying resistive layers

PERFECTLY MATCHED LAYER (PML)

Perfectly Matched Layer (PML) Formulation

The PML is composed of the following anisotropic materials:

$$\begin{cases} \bar{\bar{\sigma}}_{PML} = \bar{\bar{\Lambda}}\bar{\bar{\sigma}} \\ \bar{\bar{\epsilon}}_{PML} = \bar{\bar{\Lambda}}\bar{\bar{\epsilon}} \\ \bar{\bar{\mu}}_{PML} = \bar{\bar{\Lambda}}\bar{\bar{\mu}} \end{cases} \quad ; \quad \bar{\bar{\Lambda}} = \begin{bmatrix} \frac{\tilde{\rho}}{\rho}\frac{s_z}{s_\rho} & 0 & 0 \\ 0 & \frac{\rho}{\tilde{\rho}} s_z s_\rho & 0 \\ 0 & 0 & \frac{\tilde{\rho}}{\rho}\frac{s_\rho}{s_z} \end{bmatrix} \quad ; \quad \tilde{\rho} = \int_0^\rho s_\rho(\rho')d\rho'$$

s_ρ, s_ϕ, **and** s_z **are the stretching coordinate functions. We define:**

$$s_\rho = s_\phi = s_z = 1 + \phi - j\phi$$

We consider three different PML's by defining three different functions $\phi(x)$**:**

$$\phi(x) = \begin{cases} \phi_1(x) = \left[2\left(\frac{x - x_0}{x_1 - x_0}\right)\right]^{17} & \textbf{PML 1,} \\ \phi_2(x) = 20000\left(\frac{x - x_0}{x_1 - x_0}\right) & \textbf{PML 2,} \\ \phi_3(x) = 10000 & \textbf{PML 3.} \end{cases} \qquad x \in (x_0, x_1)$$

Within the PML, both propagating and evanescent waves become arbitrarely fast evanescent waves.

PERFECTLY MATCHED LAYER (PML)

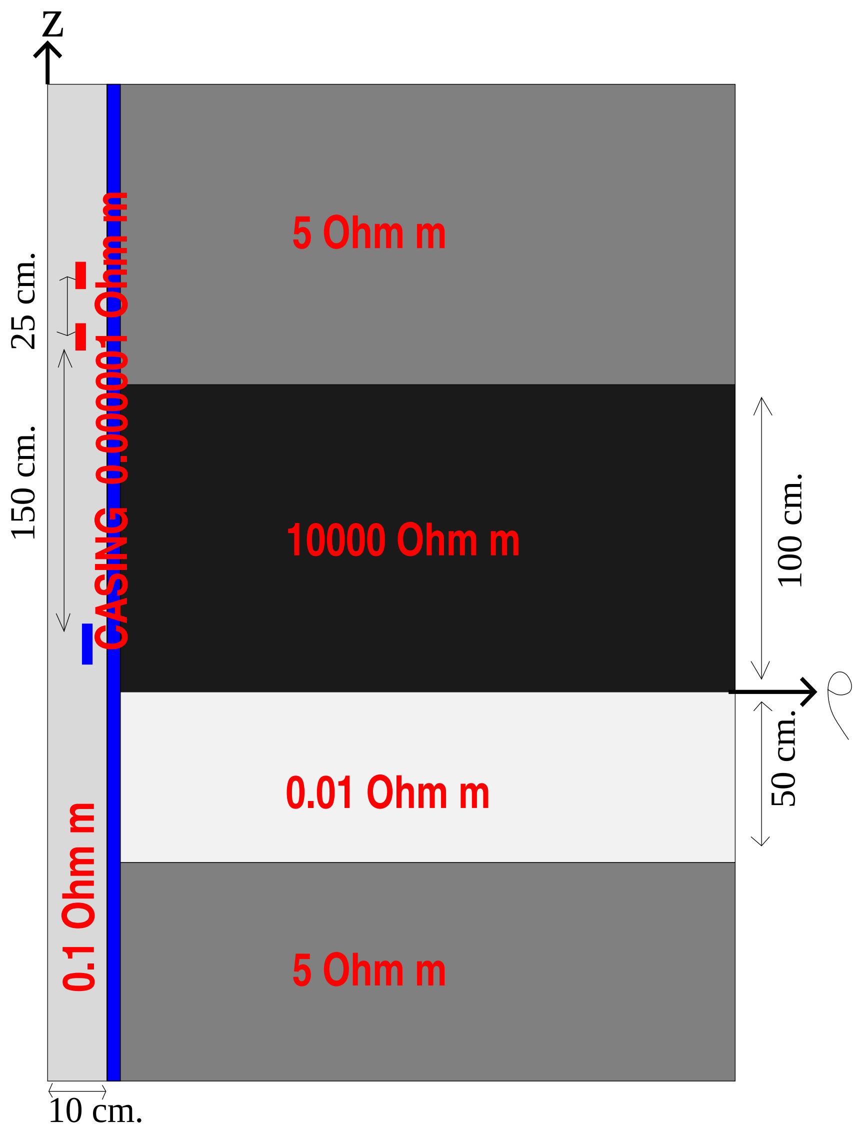

Axisymmetric 3D problem.

Six different materials.

Through casing resistivity instrument.

Varying coefficients by up to 10 orders of magnitude.

PERFECTLY MATCHED LAYER (PML)

Final hp-Grid with a 0.5 m Thick PML.

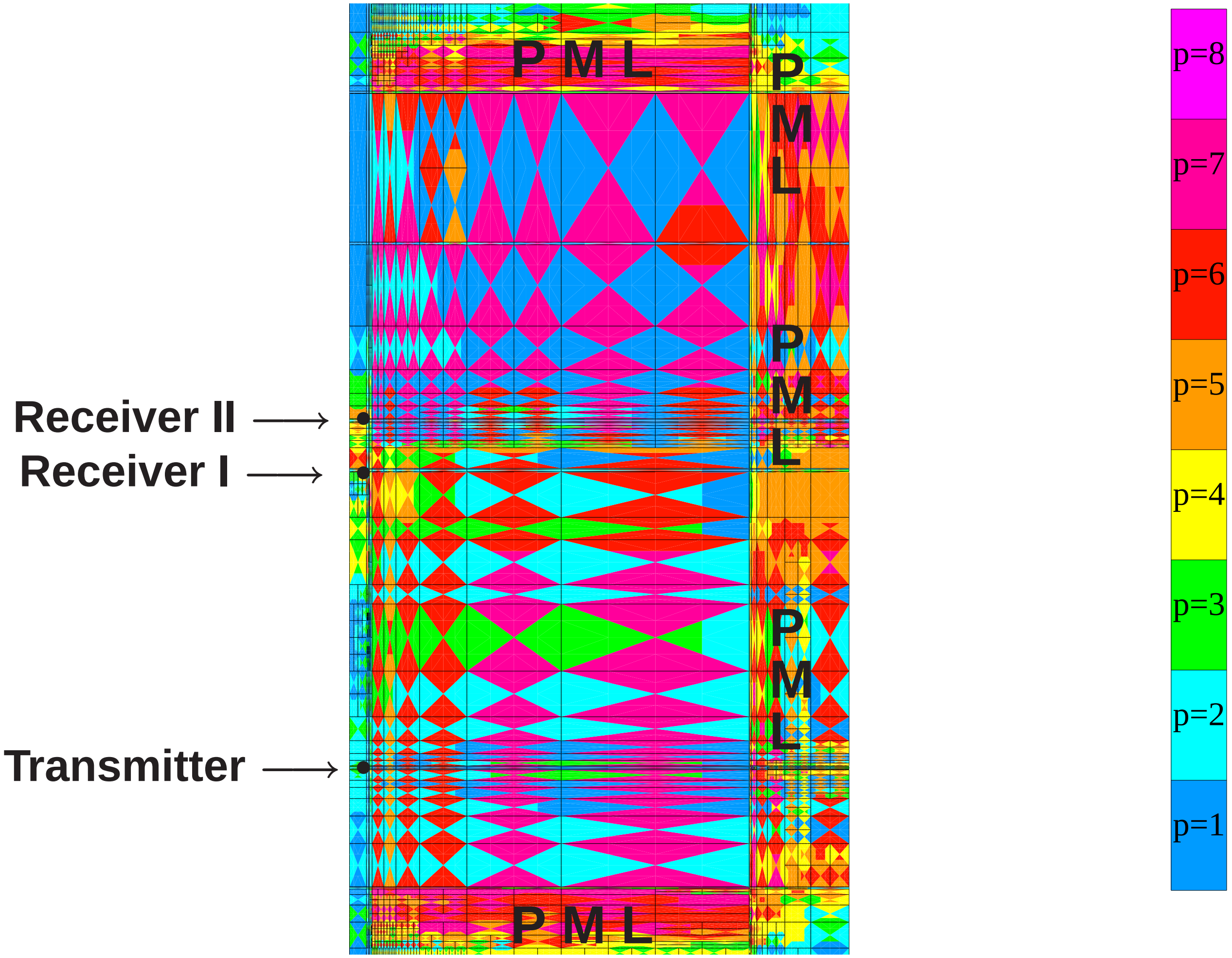

PERFECTLY MATCHED LAYER (PML)

Reference Solution: PML 1 (5 m x 2.5 m)

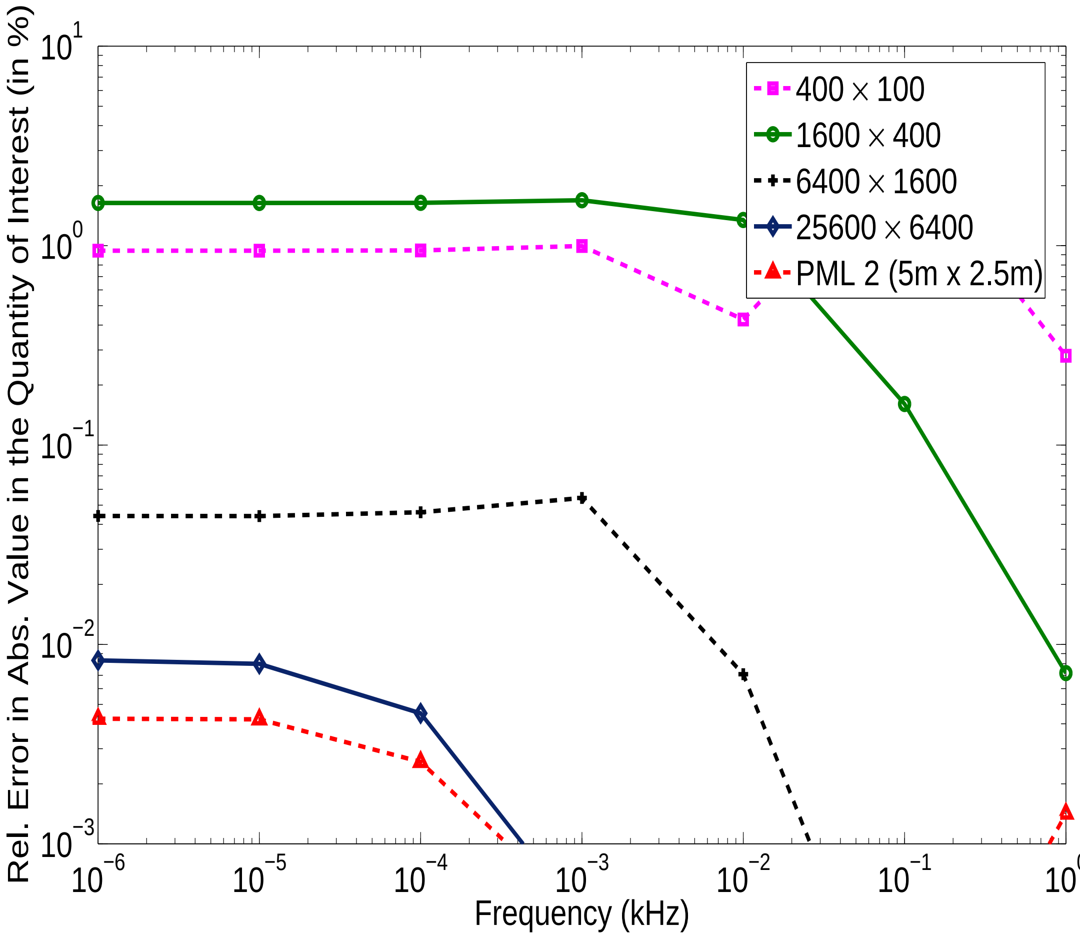

PMLs provide accurate solutions without reflections from the boundary

PERFECTLY MATCHED LAYER (PML)

Number of unknowns employed by the self-adaptive goal-oriented hp-FE method as a function of the size of computational domain and presence of a PML

Domain Size (m)	Nr. Unknowns ($\approx 1\%$ error)	Nr. Unknowns ($\approx 0.01\%$ error)
PML 1 (5 x 2.5)	19541 (0.083%)	24886 (0.037%)
PML 2 (5 x 2.5)	7095 (0.29%)	13345 (0.006%)
PML 3 (5 x 2.5)	8679 (1.04%)	19640 (0.009%)
6400 x 1600	12327 (0.43%)	18850 (0.014%)
12800 x 3200	12964 (0.43%)	18892 (0.014%)
25600 x 6400	12099 (1.22%)	19828 (0.037%)

PML 2 provides considerable savings

3D hp-FEM: NUMERICAL RESULTS (DC)

Electrode Problem

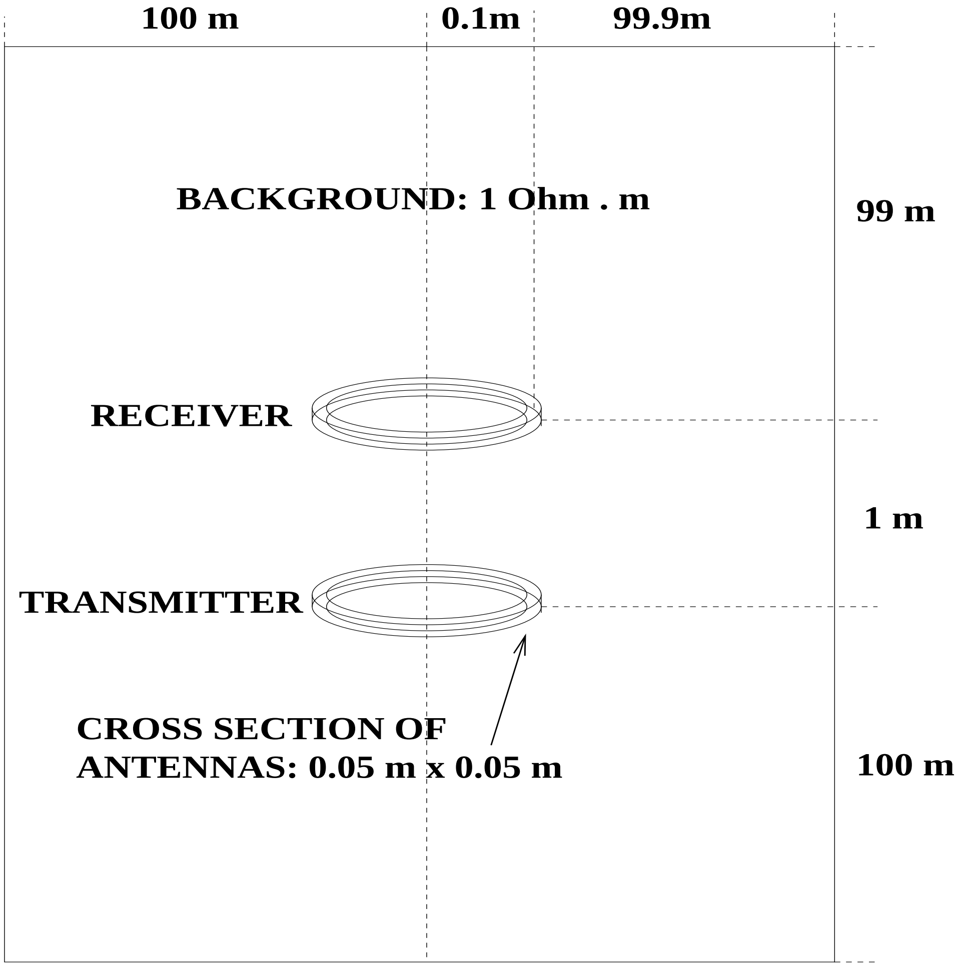

Loop antenna in a homogeneous media at DC.

Computational domain:
100 m x 100 m.

3D hp-FEM: NUMERICAL RESULTS (DC)

Electrode Problem

Final hp-grid

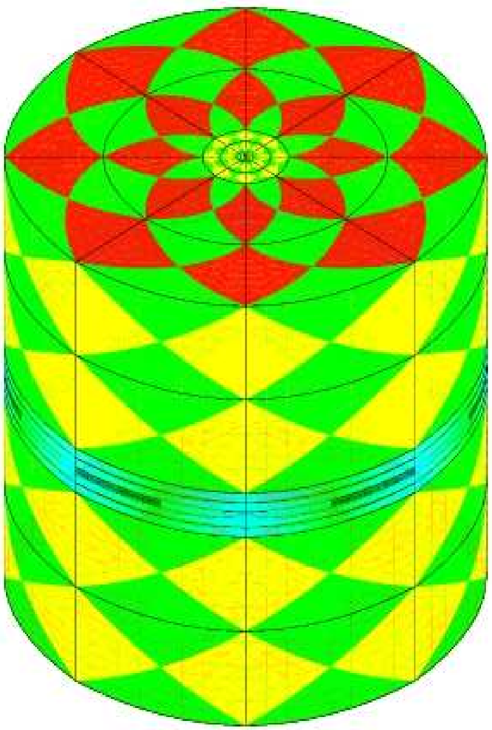

Final solution

2D Solution: 0.078131

3D Solution: 0.078121

3D hp-FEM: NUMERICAL RESULTS (DC)

Axisymmetric Model Problem

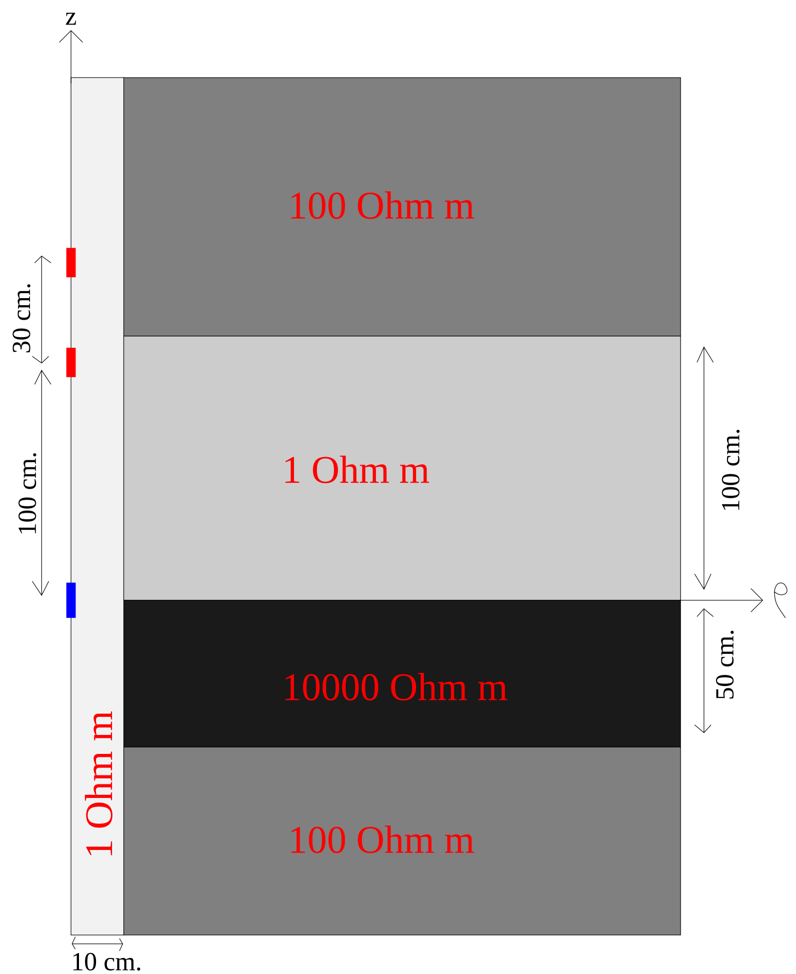

- **Borehole and four materials on the formation.**
- **Size of computational domain:** $100m \times 100m$.
- **Size of electrode:** $0.05m \times 0.05m$.
- **Objective: Compute First Vertical Difference of Potential.**

3D hp-FEM: NUMERICAL RESULTS (DC)

Axisymmetric Model Problem

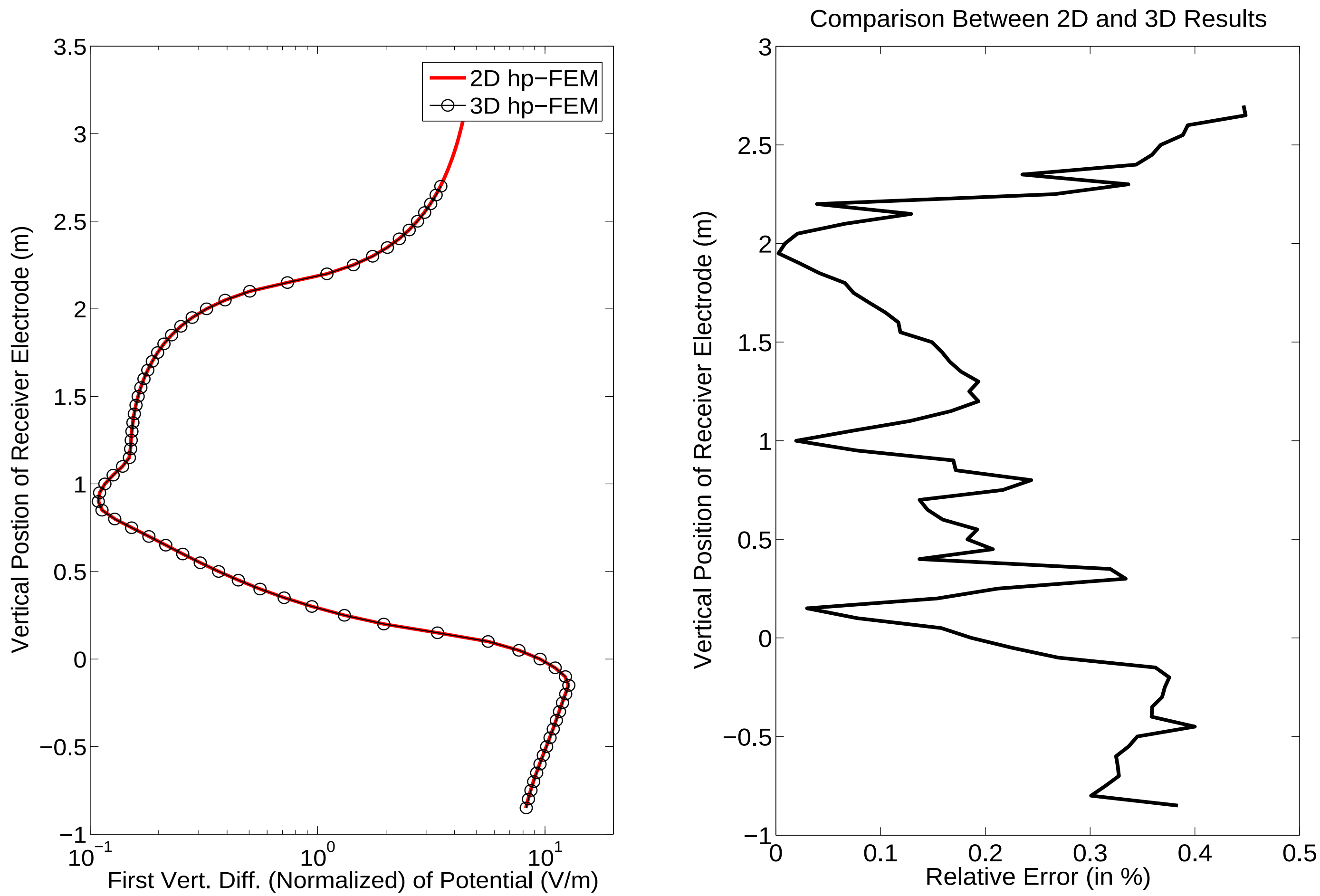

3D hp-FEM: NUMERICAL RESULTS (DC)

Axisymmetric Model Problem

MEMORY

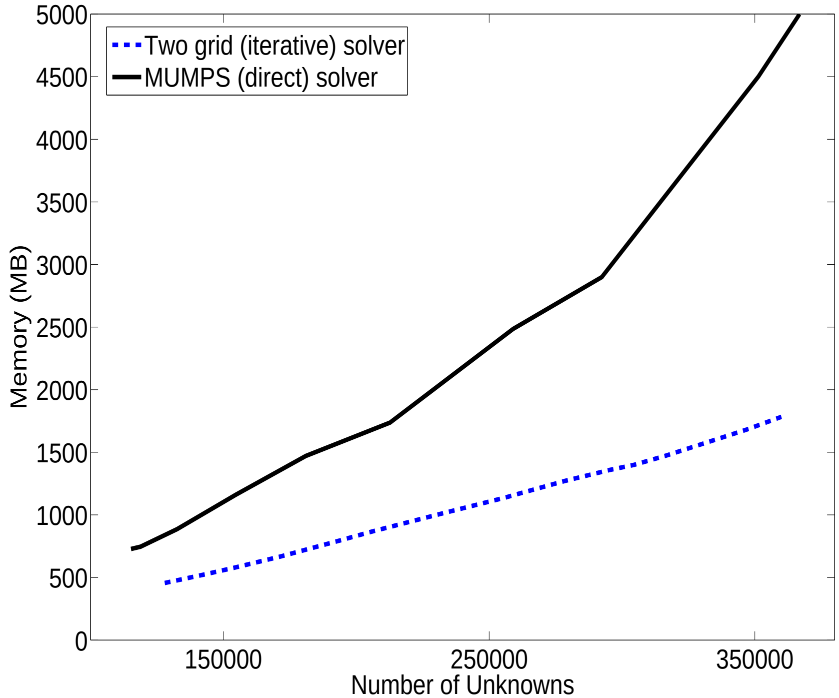

TIME

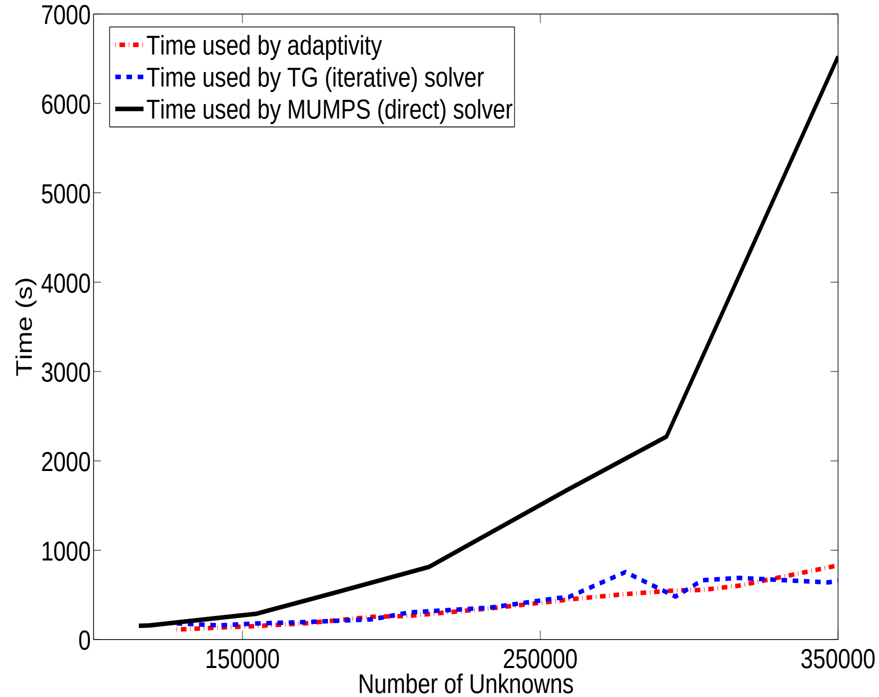

1.2 Ghz processor

Iterative solvers are needed for simulation of 3D resistivity logging applications

3D hp-FEM: NUMERICAL RESULTS (DC)

Fichera problem (unknown exact solution)

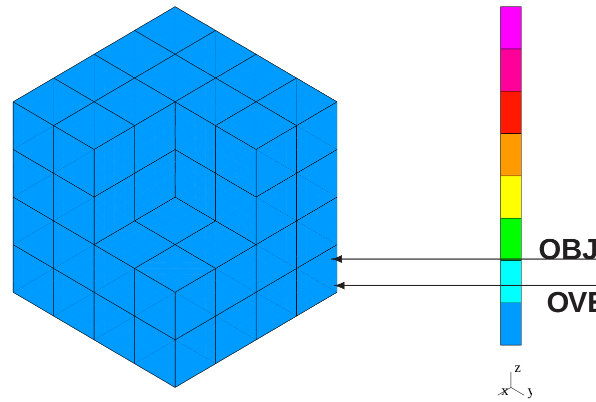

Equation: $-\Delta u = 0$
Boundary Conditions: Neumann, Dirichlet

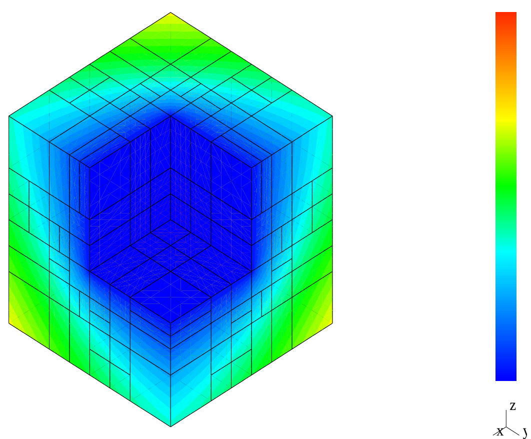

Solution of Direct Problem

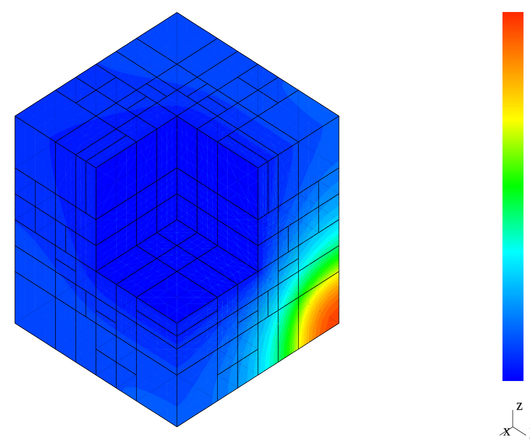

Solution of Dual Problem

3D hp-FEM: NUMERICAL RESULTS (DC)

Fichera problem (final hp-grids)

Energy-norm:

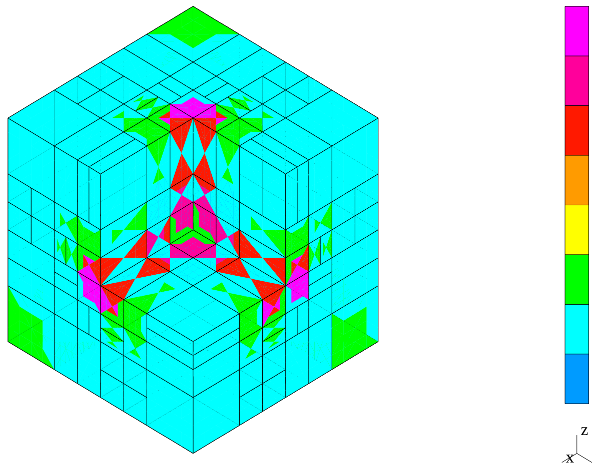

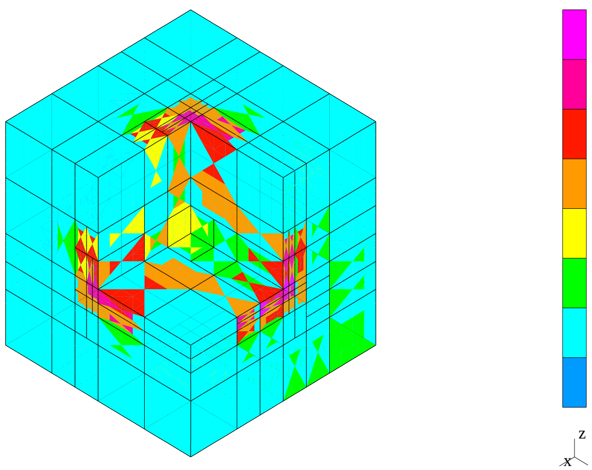

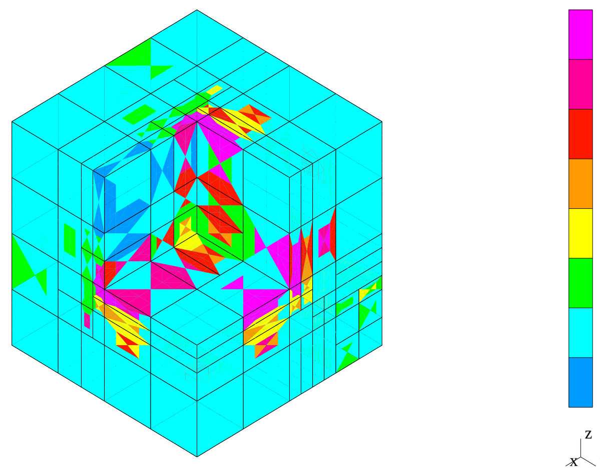

Goal-oriented (algorithm I) **Goal-oriented (algorithm II)**

3D hp-FEM: NUMERICAL RESULTS (DC)

Fichera problem (convergence history)

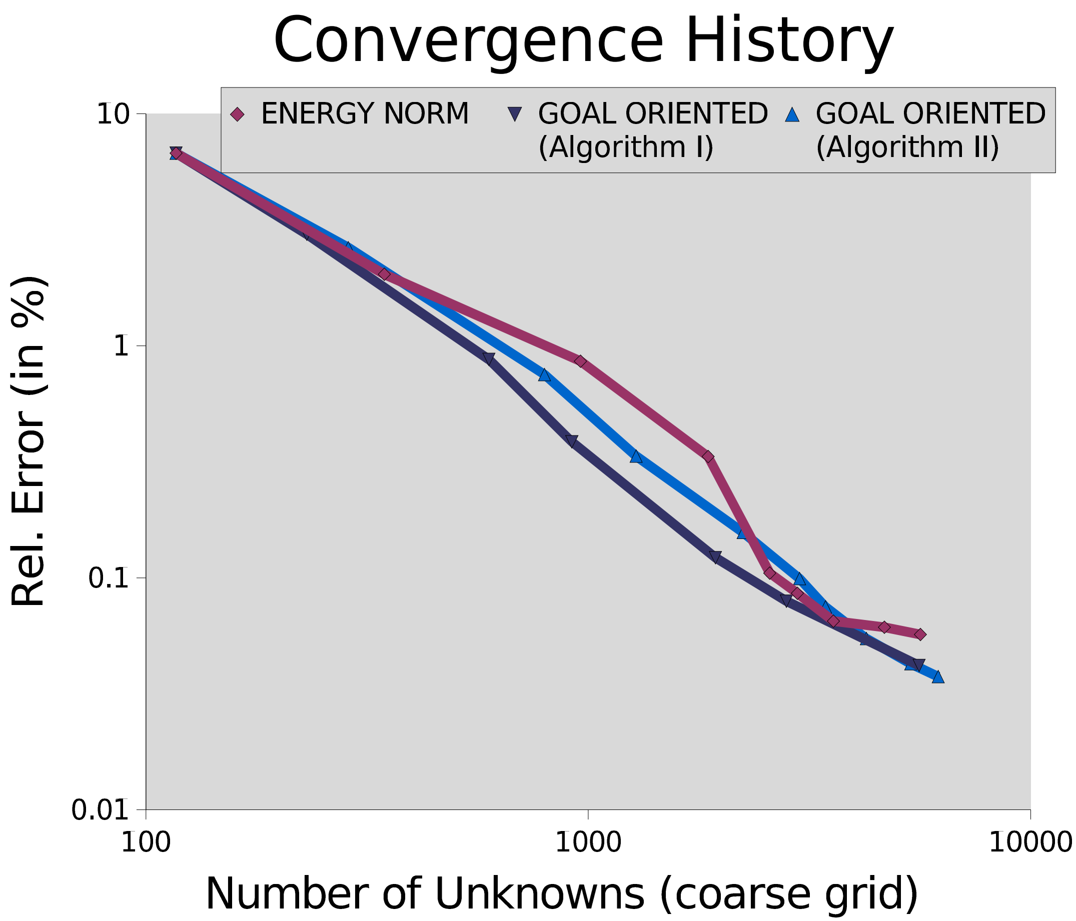

Exponential Convergence in the Quantity of Interest

CONCLUSIONS AND FUTURE WORK

- **The self-adaptive goal-oriented hp-adaptive strategy converges exponentially in terms of a user-prescribed quantity of interest vs. the CPU time.**

- **We obtain fast, reliable and accurate solutions for problems with a large dynamic range and high material constrasts.**

- **We obtain meaningful physical conclusions that are useful for instrument modeling and for assesment of petrophysical properties.**

Work in Progress

- **To further develop the parallel version of the 3D hp-FE code as well as a multigrid solver.**

- **To apply the self-adaptive goal-oriented hp-FEM for inversion of 2D multi-physic problems.**

ACKNOWLEDGMENTS

ارامكو السعودية
Saudi Aramco
BAKER HUGHES
Baker Atlas
bp
Chevron
ConocoPhillips
Agip
Eni
ExxonMobil
HALLIBURTON®
IMP Innovar
INSTITUTO MEXICANO DEL PETRÓLEO
MARATHON
Marathon Oil Corporation
HYDRO
OXY
BR PETROBRAS
Schlumberger
STATOIL
TOTAL
Weatherford